Biomedicine & Pharmacotherapy 160 (2023) 114355

Contents lists available at ScienceDirect

Biomedicine & Pharmacotherapy

journal homepage: www.elsevier.com/locate/biopha

A comprehensive pharmacological analysis of fenoterol and its derivatives to unravel the role of β_2-adrenergic receptor in zebrafish

Monika Maciag [a,b,*,1], Wojciech Plazinski [a,c,2], Wojciech Pulawski [d], Michal Kolinski [d,3], Krzysztof Jozwiak [a,4], Anita Plazinska [a,**,5]

[a] Department of Biopharmacy, Medical University of Lublin, 4a Chodzki Street, 20-093 Lublin, Poland
[b] Independent Laboratory of Behavioral Studies, Medical University of Lublin, 4a Chodzki Street, 20-093 Lublin, Poland
[c] Jerzy Haber Institute of Catalysis and Surface Chemistry, Polish Academy of Sciences, 8 Niezapominajek Street, 30-239 Cracow, Poland
[d] Bioinformatics Laboratory, Mossakowski Medical Research Centre, Polish Academy of Sciences, e Pawinskiego Street, 02-106 Warsaw, Poland

ARTICLE INFO

Keywords:
G protein-coupled receptor
Physiology
Toxicology
Anxiety behavior
Homology modeling
Zebrafish

ABSTRACT

β-adrenergic receptors (βARs) belong to a key molecular targets that regulate the most important processes occurring in the human organism. Although over the last decades a zebrafish model has been developed as a model complementary to rodents in biomedical research, the role of β_2AR in regulation of pathological and toxicological effects remains to elucidate. Therefore, the study aimed to clarify the role of β_2AR with a particular emphasis on the distinct role of subtypes A and B of zebrafish β_2AR. As model compounds selective β_2AR agonists – (*R*,*R*)-fenoterol ((*R*,*R*)-Fen) and its new derivatives: (*R*,*R*)-4'-methoxyfenoterol ((*R*,*R*)-MFen) and (*R*,*R*)-4'-methoxy-1-naphtylfenoterol ((*R*,*R*)-MNFen) – were tested. We described dose-dependent changes observed after fenoterols exposure in terms of general toxicity, cardiotoxicity and neurobehavioural responses. Subsequently, to better characterise the role of β_2-adrenergic stimulation in zebrafish, we have performed a series of molecular docking simulations. Our results indicate that (*R*,*R*)-Fen displays the highest affinity for subtype A of zebrafish β_2AR and β_{2A}AR might be involved in pigment depletion. (*R*,*R*)-MFen shows the lowest affinity for zebrafish β_2ARs out of the tested fenoterols and this might be associated with its cardiotoxic and anxiogenic effects. (*R*,*R*)-MNFen displays the highest affinity for subtype B of zebrafish β_2AR and modulation of this receptor might be associated with the development of malformations, increases locomotor activity and induces a negative chronotropic effect. Taken together, the presented data offer insights into the functional responses of the zebrafish β_2ARs confirming their intraspecies conservation, and support the translation of the zebrafish model in pharmacological and toxicological research.

1. Introduction

β-adrenergic receptors (βARs) belong to a key molecular targets that regulate the most important processes occurring in the human organism. The two endogenous ligands that stimulate the βARs are adrenaline and noradrenaline – potent and nonselective βAR agonists, which bind to the receptor, activate intracellular cyclic adenosine monophosphate signalling, trigger 'downstream' signals, and therefore promote a response from effector organs [1]. In humans, three types of βARs are distinguished – subtype β_1AR, β_2AR and β_3AR. β_1AR is predominantly located

Abbreviations: *β*-OH, *β*-hydroxyl moiety; βAR, β-adrenergic receptors; TM, transmembrane domain; LC_{50}, half-maximal lethal concentration; HB, hydrogen bond; hpf, hours post-fertilisation; COI, compound of interest; *R,R*-MNFen, (*R*,*R*)-4'-Methoxy-1-naphtylfenoterol; *R,R*-MFen, (*R*,*R*)-4'-Methoxyfenoterol; *R,R*-Fen, (*R*,*R*)-Fenoterol; *R,R*/S,S-Fen, (*R*,*R*)/(*S*,*S*)-Fenoterol.

* Corresponding author at: Department of Biopharmacy, Medical University of Lublin, 4a Chodzki Street, 20-093 Lublin, Poland.
** Corresponding author.
E-mail addresses: monikamaciag@umlub.pl (M. Maciag), anita.plazinska@umlub.pl (A. Plazinska).
[1] ORCID 0000-0002-9866-9612.
[2] ORCID 0000-0003-1427-8188.
[3] ORCID 0000-0003-1047-2186.
[4] ORCID 0000-0001-6018-5092.
[5] ORCID 0000-0002-3698-2574.

https://doi.org/10.1016/j.biopha.2023.114355
Received 8 November 2022; Received in revised form 30 January 2023; Accepted 31 January 2023
Available online 3 February 2023

in the area of the heart [2], β_2AR is distributed in the pulmonary, cardiovascular, digestive, reproductive and central nervous systems [3], whereas β_3AR distribution is mainly limited to adipose tissue and the gastrointestinal tract [4]. The β_2AR stimulation causes smooth muscle relaxation, which may result in bronchodilation, as well as vasodilation of uterine and liver muscles [5]. The clinical use of drugs that act on β_2AR is effective in a range of pulmonary diseases, including asthma and chronic obstructive pulmonary disease, and there is no comparable alternative to treat patients. What is more, β_2AR has been extensively studied as a new potential target for the therapy of complex disorders, including heart disease [6], cancer [7,8], diabetes [9], obesity [10], as well as its neuroprotective [11] and anti-inflammatory [12,13] properties have been demonstrated. Significant progress was recently made towards answering the question on the role of stimulation of β_2AR in cardioprotection [2]. Although the hypothesis that β_2AR can be contributed to cardioprotection initially seemed surprising, since adrenaline and noradrenaline were well-known to induce toxic effects on the heart, i.e. an excessive level of catecholamines induces myocardial destruction, reduces myocyte number and increases cardiomyocyte necrosis [14], further studies demonstrated that a knock-out of β_2AR even exacerbated mortality and cardiomyocyte apoptosis in response to catecholamine stimulation in rodents [6]. Detailed research elucidating the switching role of βARs in cardiotoxicity/cardioprotection summed that β_1AR is mainly involved in cardiotoxicity, whereas β_2AR takes part in cardioprotection [15]. On the other hand, in recent years there has been a growing interest in the potential use of β_2AR agonists for cancer management. β_2AR modulation was proved effective against melanoma [16], pancreatic [17] and glioma [18] cell lines mortality and motility. Therefore, these dual therapeutic effects of β_2AR agonists, i.e. cardioprotective and antitumor, can be helpful, in particular, in the new emerging field of the cardio-oncology.

As β_2AR has arisen as a promising molecular target for the therapy of a broad set of disorders, the new sub-type selective β_2AR agonists were synthesised and tested for the β_2AR activity and selectivity [19]. The most selective β_2AR agonists with a complex pharmacological profile are fenoterol and fenoterol derivatives. Fenoterol has been shown to have 97.7 times higher selectivity for the human β_2AR than for β_1AR and 43.7 times higher selectivity for β_2AR than for β_3AR [20]. Nevertheless, along with a dose-related loss of β_2AR selectivity, fenoterol is able to cross--react with β_1AR and β_3AR. It is often assumed that the side effects of β_2AR agonists are associated with drug overdose due to the stimulation of β_1AR [5]. It has been also shown that fenoterol stimulates the β_3AR and the selective β_3AR antagonist – L-748,337 – is able to block this activation [21]. However, comparing a selective β_2AR antagonist – ICI-118,551 – with the selective β_3AR antagonist, the former one is more potent as a fenoterol blocker [22]. Although (*R*,*R*)/(*S*,*S*)-fenoterol ((*R*,*R*)/(*S*,*S*)-Fen) is clinically used in the therapy of asthma, its administration is limited by cardiac adverse events, including myocardial repolarisation abnormalities observed in vitro [23] and in clinical [24] studies. As mentioned before, for the reason that β_1AR is mainly implicated in cardiotoxicity, searching for more selective β_2AR stimulants was conducted, concluding that the methoxy group and the aromatic moiety on the aminoalkyl region of the fenoterol molecule contribute to increasing β_2AR subtype selectivity [25]. Additionally, Jozwiak and colleagues [26] highlighted a significant role of fenoterol's stereochemistry on the β_2AR system's activation. Even though from a chemical perspective enantiomers elicit similar properties, this enantiomeric specificity might be crucial for agonist-mediated functional responses from the stimulated receptor [5]. These discoveries led to the synthesis of new compounds, among many these were: (*R*,*R*)-fenoterol ((*R*,*R*)-Fen), (*R*,*R*)-4'-methoxyfenoterol ((*R*,*R*)-MFen) and (*R*,*R*)-4'-methoxy-1-naphtylfenoterol ((*R*,*R*)-MNFen).

β_2AR can signal either through G proteins or through β-arrestin [27,28] and there are several groups of ligands that are able to activate different signalling patterns; for instance, paths acting through different G proteins, G protein vs β-arrestin or are biased from other signalling readouts [27,29]. Importantly from the cardiovascular research standpoint, it has been shown that the inhibitory G_i signalling of β_2AR becomes exaggerated in heart failure causing various adverse structural and functional consequences in the heart [29]. On the other hand, β-arrestin has been shown to be cardioprotective, as it inhibits apoptosis, inflammation and attenuates adverse cardiac remodelling [28]. Therefore, the development of novel drugs that show biased agonism towards the stimulatory G_s or β-arrestin might have new therapeutic potential. (*R*,*R*)-Fen, (*R*,*R*)-MFen and (*R*,*R*)-MNFen differ in relation to their selectivity towards the G proteins (stimulatory G_s and inhibitory G_i). A previous study showed that (*R*,*R*)-Fen and (*R*,*R*)-MFen belong to G_s-biased β_2AR agonists, whereas (*R*,*R*)-MNFen is unbiased in terms of β_2AR-G_s/G_i signalling, i.e. couples both G_s and G_i protein to β_2AR [30]. The continuation of this study was to characterise the β-arrestin-biased agonism of β_2AR for (*R*,*R*)-Fen and (*R*,*R*)-MNFen, among many other compounds [29]. Woo and co-authors [29] showed that (*R*,*R*)-Fen and (*R*,*R*)-MNFen activate G_s slightly stronger than β-arrestin, but the ligand biases for these proteins have no difference compared with that of (*R*)-isoprenaline, a non-biased agonist of β_2AR used as the reference compound. In spite of the fact that the fenoterol and its derivatives have been extensively studied to define their pharmacological properties, especially in the management of heart disease and cancer [6], it still remains unclear how they affect a whole body, and what undesirable effects on living organisms we could expect.

In recent years, a zebrafish (*Danio rerio*) model has emerged as a powerful system to evaluate the effects of new compounds during the initial phase of the drug discovery process [31,32]. External fertilisation, small size and optical transparency allow for phenotypic screening of thousands of embryos in a living whole animal. This provides a significant advantage for zebrafish, since permits screening on a scale beyond what is now available in the other vertebrate models. Zebrafish shares 70 % of their genome with humans, and above 80 % of human disease genes have a counterpart in zebrafish [33]. Molecular pathways, receptors and enzymes are analogous between zebrafish and humans, which provides an intraspecific conservation of the functional activity of drugs. Evidence from more than 20 years of zebrafish-based drug screenings confirms that the zebrafish model can be successfully used to recognise new therapeutic candidates, e.g. leflunomide, an agent identified in zebrafish, is in phase I of a clinical study to treat melanoma [31], and to model a wide array of diseases, including heart failure, cancer, liver disease, inflammation and psychiatric disorders [34]. Another unique advantage is that zebrafish are characterised by rapid development during early embryonic stages. The development of most organs is mostly completed between 48 and 72 h post-fertilisation (hpf). Heart beating and blood flow circulation is initiated as early as 24 hpf [35], and the first spontaneous movements appear around 18 hpf [36], and are further turned into complex swimming repertoires, e.g. locomotor response within 96 hpf. While embryonic zebrafish were initially used for the evaluation of environmental contaminants in toxicological studies, in recent years increasing numbers of research have focused on the use of zebrafish in the field of pharmaceutical toxicology, confirming interspecies translation of this model [37–39].

Little is known about the β_2AR system in zebrafish so far. Catecholaminergic cells are observed in zebrafish embryos as early as 24 hpf [40]. Five βARs were distinguished; one β_1AR, two distinct β_2ARs (herein termed β_{2A}AR and β_{2B}AR) and two distinct β_3ARs (β_{3A}AR and β_{3B}AR) [41]. The zebrafish β_2ARs are two distinct proteins encoded by genes *adrb2a* (location: chromosome 14) and *adrb2b* (location: chromosome 21). Both type of zebrafish β_2ARs are orthologous to the human β_2AR [41]. An important difference between forms A and B of β_2ARs in zebrafish is the expression profile; type A of β_2ARs is highly expressed in the brain and skin, whereas type B is predominant in skeletal muscle, liver and pancreas. In regard to other zebrafish receptors, β_1AR is expressed abundantly in the brain, heart and eye, whereas β_3ARs are restricted to the blood [41]. Both β_2ARs variants are involved in the regulation of cardiac functions; however, they may have specific

functions. While β_1AR and β_2ARs are able to initiate the stimulatory G_s protein, one or both zebrafish β_2ARs may reduce cardiac functions by interacting with the inhibitory G_i protein [42]. Furthermore, the involvement of β_2ARs has been highlighted in neuropharmacological studies in zebrafish [43]; type A of zebrafish β_2ARs may be able to regulate the development of pigmentation [41] and the role of β_1AR and β_{2B}AR during body axis straightening was recently pointed out by Wang and co-authors [44].

In our study, we have evaluated the toxicological and pharmacological effects of selective β_2AR agonists, i.e. (*R*,*R*)-Fen, (*R*,*R*)-MFen and (*R*,*R*)-MNFen in embryonic zebrafish, which are parallel in respect to enantiomeric specificity. Here, we described the whole organism changes observed after these drugs' exposure in terms of general toxicity, cardiotoxicity, and neurological and behavioural responses. Subsequently, to better characterise the role of β_2-adrenergic stimulation in zebrafish, we have performed a series of molecular dockings aimed at elucidating the molecular details of interactions between the two subtypes of zebrafish β_2AR and ligands binding them, i.e. both the fenoterol, fenoterol derivatives and β_2AR agonists ((*R*)-adrenaline, BI-167107 and (*R*,*R*)-formoterol).

2. Material and methods

2.1. Preparation of drugs

Chemicals were prepared in the zebrafish medium (pH 7.1 – 7.3; 5.0 mM NaCl, 0.17 mM KCl, 0.33 mM CaCl2, 0.33 mM MgSO4) and diluted to the final test concentrations immediately prior to the experiments. (*R*,*R*)-Fen, (*R*,*R*)-MFen and (*R*,*R*)-MNFen were synthesised as described previously [25]. The chemical structures of the tested compounds are depicted in Fig. 1A.

2.2. Zebrafish maintenance

Zebrafish (*Danio rerio*) embryos were provided by the animal facility at the Experimental Medicine Center, Medical University of Lublin, Poland. Adult, AB strain was maintained at 28.5 °C, on a 14:10 h light/dark cycle under standard aquaculture conditions. Zebrafish embryos were collected following natural mating.

2.3. Ethics declarations

All experiments were conducted in accordance with the National Institute of Health Guidelines for the Care and Use of Laboratory Animals and the European Community Council Directive for the Care and Use of Laboratory Animals of September 22, 2010. All methods involving zebrafish embryos were in compliance with Animal Research: Reporting of In Vivo Experiments (ARRIVE) guidelines. For the experiment with larvae up to 120 hpf, the agreement of the Local Ethical Committee is not required.

2.4. Chemical treatment

The toxicity of chemical substances was assessed using the zebrafish model according to modified OECD Guidelines for the Testing of Chemicals [45]. The experimental design scheme is depicted in Fig. 2A. At least 48 embryos per treatment group were randomly selected and transferred to 6-well plates filled with 2 mL of the compound of interest (COI) in gradient concentration and control solution (negative) not later than 90 min post fertilisation. Embryos were investigated under a light microscope, and 24 viable fertilised embryos were selected and transferred to 96-well plates within 3 hpf. Embryos were individually incubated in 200 μL of COI or control solution. Working solutions of the drugs were refreshed every 24 h. The embryos were exposed to 'control' or 'treatment' solutions up to 96 h. Plates were kept at 28.5 ± 0.5 °C with a 14:10 h light/dark cycle. Immediately after the experiment, larvae were euthanised by immersion in the overdose of 15 μM tricaine methanesulfonate (MS-222) solution (Sigma-Aldrich). Experiments were performed in two cohorts. Experiments on every cohort were carried out at least one week apart. Within each cohort, there were two batches of embryos obtained during two independent matings.

2.5. Toxicity assessment

Developmental toxicity endpoints were examined every 24 h, up to 96 hpf. At 96 hpf, the number of dead embryos was scored and LC_{50} (lethal concentration, 50 %) values were generated for each drug. At 24 hpf death was judged by coagulation of embryos, while at later timepoints also by the absence of the heartbeat and the lack of movement observed for 20 s. Dead embryos were discarded. A test was considered valid when the mortality in the negative control did not exceed 10 %.

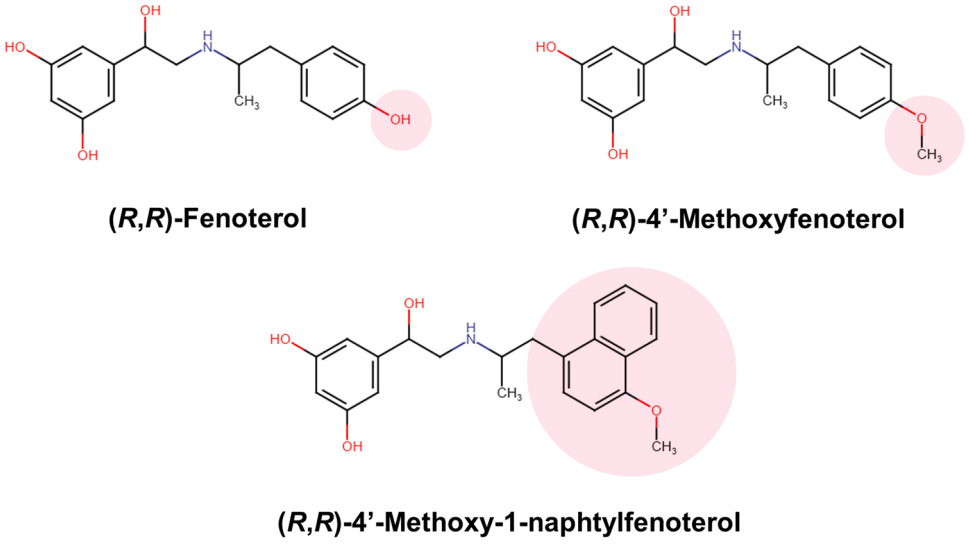

Fig. 1. Chemical structures of fenoterol and fenoterol derivatives. Chemical structure of (*R*,*R*)-fenoterol ((*R*,*R*)-Fen), (*R*,*R*)-4'-methoxyfenoterol ((*R*,*R*)-MFen) and (*R*,*R*)-4'-methoxy-1-naphtylfenoterol ((*R*,*R*)-MNFen). The chemical structures were drawn in a free online Chem-Space tool (chem-space.com).

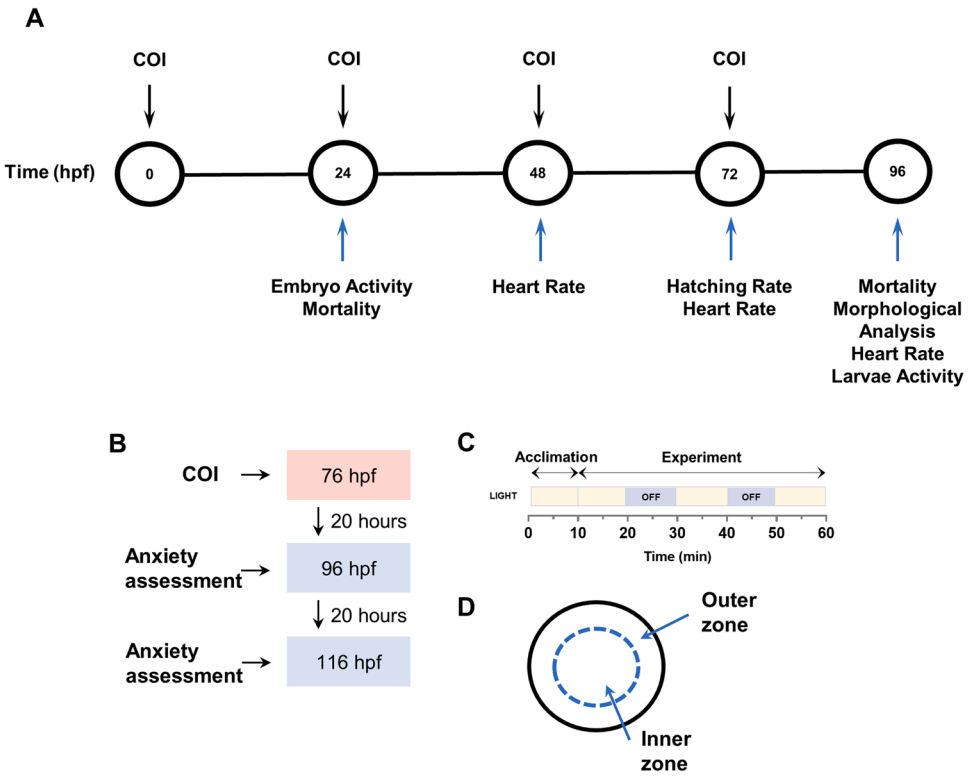

Fig. 2. Experimental design scheme for zebrafish treatment with fenoterol and its derivatives in zebrafish. Animals were exposed to compounds of interest (COI) every 24 h, starting immediately after fertilisation (hpf). The last treatment was performed at 72 hpf. Mortality dose-response curves were generated for data obtained at 24 and 96 hpf. Spontaneous coiling activity was monitored in 24 hpf embryos. Heart rate was analysed at 48, 72 and 96 hpf. Hatching and morphological abnormalities were examined in fish at 72 hpf and 96 hpf, respectively. Distance and velocity swam by larvae were examined after 96 after of exposure to COI (A). To assess anxiety-like behaviours larvae were exposed to COI starting from 76 hpf. Behavioural analyses were performed at two distinct time points, i.e. 96 hpf and 116 hpf (B). The anxiety-related behaviour was assessed under the light-dark transition test. The first 10 min were an acclimatisation phase, and then equal 10 min of light and dark challenging periods were an experimental procedure (C). Thigmotaxis was used as an indicator of anxiety-like behaviour in larvae (D).

2.6. Morphological analysis

Larvae were assessed morphologically using a light microscope (Zeiss Stemi 508 microscope) throughout the experiment. The percentage of cardiac abnormalities (pericardial oedema, stretched heart, haemorrhage and/or impaired blood flow) was determined at 96 hpf, as the ratio of abnormal zebrafish over the number of alive zebrafish. Other types of malformations including head malformation, tail malformation, growth retardation and pigment depletion were also scored. For imaging, zebrafish larvae were immobilised on 3 % methylcellulose, and the photos were captured using Zeiss SteREO Discovery.V8 microscope.

2.7. Heart rate assessment

Heart rate was measured in 5 randomly selected larvae per treatment. At 48 hpf and 72 hpf, the heartbeats were counted under a stereomicroscope (Zeiss Stemi 508 microscope) for 20 s. At 96 hpf, the animals were immobilised on 3 % methylcellulose (Sigma-Aldrich). The heart was recorded using an AxioCam camera for 20 s per animal (Zeiss SteREO Discovery.V8 microscope). Heartbeat videos were then analysed using the DanioScope (Noldus, Wageningen, the Netherlands) software.

2.8. Motor activity measurement

24 hpf embryos were embedded in low melting agarose and their movements inside the chorion were recorded using an AxioCam camera (Zeiss SteREO Discovery.V8 microscope) for 20 min. The Danioscope software was used to quantify the percentage of total time during which the embryos were active [46]. At 96 hpf larvae were transferred individually into a 96-well plate and locomotor activity was recorded for 10 min using Basler GenlCam [acA1300–60] camera and DanioVision recording chamber. Analyses were performed using the Ethovision XT 15 software (Noldus, Wageningen, the Netherlands) to quantify the distance swam and velocity under lightening conditions.

2.9. Anxiety-related behaviour assessment

To further evaluate the neuroactive properties of the fenoterol compounds, zebrafish larvae were exposed acutely to the compounds starting from 76 hpf (Fig. 2B). 24 larvae per treatment group were randomly selected and transferred to 24-well plates filled with 1 mL of the COI in gradient concentration and control solution (negative). The concentrations were selected based on the toxicological studies, i.e. non-toxic doses of 1/100, 1/1000 and 1/10000 of LC_{50} for each compound were tested. Zebrafish were tested in two separate time points: after 20 (96 hpf) and 40 (116 hpf) hours of exposure. By 96 hpf – 120 hpf, larvae start to exhibit an array of behaviours, e.g. phototaxis and thigmotaxis, and therefore are useful for testing numerous neurobehavioral endpoints [47–49]. The same fish were used in both experiments. To minimise stress from the behavioural procedure, the experiments were conducted out within 20 h intervals. Working solutions of the drugs were refreshed every 20 h. The anxiety-related behaviour was assessed under the light-dark transition test (Fig. 2C). The first 10 min were an acclimatisation phase, and then equal 10 min of light and dark challenging periods were an experimental procedure: light-dark-light-dark-light. Thigmotaxis was used as an indicator of anxiety-like behaviour in larvae. The percentage of the total distance moved in the inner zone over the whole area of the well under dark phases was used to assess the level of anxiety in fish according to Schnorr and colleagues [50] with a small modification. The changes in anxiety level were only assessed under dark condition since fish at this developmental stage do not display adequate and stable level of behavioural exploration under basal conditions [50]. General locomotor activity was measured as the total distance moved per one minute time bin, under different light on/off conditions. Animals were recorded using Basler GenlCam [acA1300–60] camera and DanioVision recording chamber and analyses were performed using the Ethovision XT 15 software (Noldus, Wageningen, the Netherlands).

2.10. The involvement of β_2ARs in the observed effects of the fenoterol compounds

To evaluate whether the fenoterol compounds act through β_2ARs also in zebrafish, zebrafish larvae were co-treated with (*R*,*R*)-Fen and a highly selective β_2AR antagonist: ICI-118,551 hydrochloride (Cayman Chemical) and the changes in heart rate were examined. 72 hpf zebrafish larvae were exposed to (*R*,*R*)-Fen for 24 h. Pre-treatment of zebrafish with ICI-118,551 or control solution was conducted two hours prior to (*R*,*R*)-Fen exposure.

2.11. Statistical analysis

For statistical analysis, nonlinear regression was performed on dose-response mortality data. Four parameters sigmoidal curve was used for the calculation of concentration that was lethal to 50 % of the animals (LC_{50}). Normality was tested using D'Agostino-Pearson omnibus K2 method. F and Brown-Forsythe tests were used to compare variances between two and more groups, respectively. Hatching rate, morphological abnormalities and heart rate data were analysed using a two-way analysis of variance followed by Bonferroni's post-hoc test. Heart rate data and behavioural data were analysed using a one-way analysis of variance followed by Tukey's post-hoc test. Kruskal-Wallis test with Dunn's posthoc test was used for datasets that failed normality testing or had significantly different variances. The confidence limit of $p < 0.05$ was considered as statistically significant. Data were presented as mean or mean ± the standard deviation (SD). All analysis was carried out using Prism v8.3.1 from GraphPad software.

2.12. Receptor structures

Molecular models for subtype A and subtype B of β_2AR of zebrafish were created using comparative modelling techniques. The amino acid sequences for the two target receptor subtypes were obtained from the UniprotKB database [51], identifiers: I7GPU6 (length 405) for b2-adre-A (β_{2A}AR) and F1QBF9 (length 405) for b2-adre-B (β_{2B}AR), respectively. To predict the structures of target receptors in their active conformations, two experimental structures of the human β_2AR-G_s protein complex with bound agonist were chosen as templates: PDB IDs: 3SN6 [52] and 7BZ2 [53], respectively. In both selected structures receptor presented a fully active conformation. The selected targets included an incomplete ICL3 structure. The loop coordinates were taken from the structure of the nanobody-stabilised active state of the human β_2AR, PDB ID: 3P0G [54] (chain fragment form Ala174 to Asn196) after structural superimposition of receptor structures. The multiple sequence alignment of amino acid sequences of the two template proteins and the two targets was performed using ClustalW program [55]. The alignment was manually optimised in the intracellular loop regions. The homology modelling procedure was conducted using Modeller ver. 10.1 [56] resulting in the two distinct molecular models for each receptor subtypes: A and B.

2.13. Ligand-receptor docking

Molecules of studied ligands ((*R*)-adrenaline, BI-167107, (*R*,*R*)-formoterol, (*R*,*R*)-Fen, (*S*,*S*)-Fen, (*R*,*R*)-MFen and (*R*,*R*)-MNFen) were drawn manually by using the Avogadro 1.1.1 software [57] and optimised within the UFF force field [58] (5000 steps, steepest descent algorithm). Optimised ligands were docked to the four homology models of type A and B of zebrafish β_2AR, based on two crystal structures of human β_2AR (see the previous subsection). The docking simulations were carried out by using the AutoDock Vina software [59]. The procedure of docking was carried out within the cuboid region of dimensions of $20 \times 20 \times 20$ Å^3 which covers all the originally co-crystallised ligands present in the original PDB structures as well as the closest amino-acid residues that exhibit contact with those ligands. All the default procedures and algorithms implemented in AutoDock Vina were applied during docking. In addition to the flexibility of the ligands molecules the residues created the binding site was allowed to rotate as well. In addition to compounds considered in the experimental part of the study, the three further ligands were considered in order to comparison of their binding characteristics with those corresponding to the available resolved structures of human β_2AR-ligand complexes: BI-167107 (PDB: 3SN6) [52], (*R*,*R*)-formoterol (PDB: 7BZ2) [53] and (*R*)-adrenaline (PDB: 4LDO) [60].

3. Results

3.1. Negative control group

The mortality and spontaneous malformations in the negative control group did not exceed 10 % (data not shown).

3.2. Toxicological assessment of fenoterol and its derivatives

Overdose of the drugs that stimulate the β-adrenergic system affects in particular the cardiovascular and neuromotor systems in humans. β_2AR agonists applied at higher doses lose their selectivity for β_2AR, and therefore β_1AR-related effects may be observed, leading to the impairment of cardiac functions, skeletal muscle tremors and an increase in anxiety level [5]. Since toxicity endpoints directly depend on exposure level [61], we decided to perform complete dose-response analyses of the pharmacological and toxicological effects, e.g. mortality rate, developmental malformation, cardiotoxic and neurotoxic properties, of fenoterol and its derivatives in embryonic fish.

3.2.1. (R,R)-Fenoterol displayed the lowest mortality rate

The first tested compound – (*R*,*R*)-Fen elicited a 50 % lethality (LC_{50}) at the concentration equal to 5.58 mM, after 96 h of exposure (Fig. 3A). A significant delay in the hatching rate was observed at the doses of 5.0 mM and 10.0 mM (Fig. 3B). Interestingly, (*R*,*R*)-Fen substantially suppressed the development of pigmentation (Fig. 3C). Representative photos are provided in Supplemental Information (Fig. S1A). However, the effect was associated with both mentioned toxicity endpoints, i.e. an increase in mortality and inhibition in hatching rate. The dose- and time-ranging heart rate analysis revealed that (*R*,*R*)-Fen did not affect the heart rate at 48 hpf, and only later significantly increased the heart rate at the lowest tested dose of 0.01 mM at 72 hpf. As expected, the heart rate decreased with a further increase in the compound concentrations. (*R*,*R*)-Fen reduced heart rate in the doses above 2.5 mM at 72 hpf. The effect was maintained at the doses of 2.5 mM and 5.0 mM at 96 hpf (Fig. 3D). (*R*,*R*)-Fen enhanced locomotor activity in 24 hpf embryos up to the doses of 0.25 mM, indicated by an increase in the percentage of total time during which the embryos were active (Fig. 3E). The effect was followed by a reduction in the coiling activity. As a result of this inhibitory effect, the motor activity returned to baseline at the sub-lethal dose of 5.0 mM. The tested compound changed no distance (Fig. 3F) nor velocity (Fig. 3G) swam by larvae after prolonged 96 h of exposure.

3.2.2. (R,R)-4'-Methoxyfenoterol reduced heart rate at a wide range of concentrations

Toxicological assessment of the next tested fenoterol derivative – (*R*,*R*)-MFen showed that the compound displayed similar lethality resulting in an LC_{50} value equal to 5.21 mM (Fig. 4A). (*R*,*R*)-MFen significantly reduced the hatching rate at 10.0 mM (Fig. 4B). In contrast to the parent compound, (*R*,*R*)-MFen did not affect morphological development, including pigmentation (Fig. 4C and Fig. S1B). Regarding cardiac changes, the heart rate was increased at the dose of 0.1 mM (Fig. 4D) after 24 h of exposure. With an increase in doses, heart rate returned to baseline and significantly dropped at 2.5 and 5.0 mM. The effect was sustained over 72 hpf at 5.0 mM. At 96 hpf, the compound reduced heart rate at a wide range of concentrations between 0.25 mM and 5.0 mM. 24

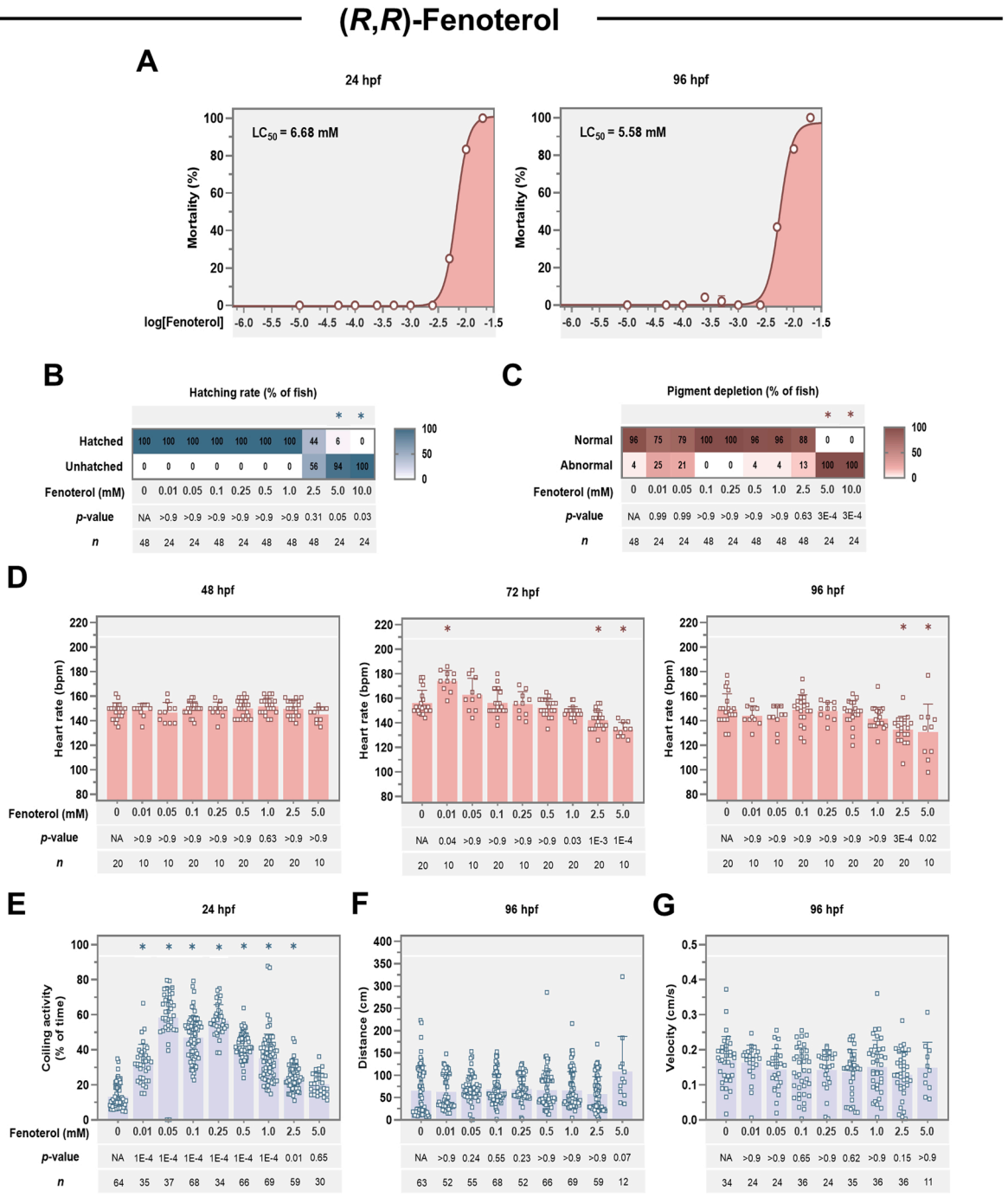

Fig. 3. Toxicity and activity of (*R*,*R*)-fenoterol in zebrafish. Effects of (*R*,*R*)-Fen on the mortality (A), hatching rate (B), morphological changes (C), heart rate (D), coiling activity (E), distance (F) and velocity (G) swam by larvae. Nonlinear regression was performed on dose-response mortality data (A) at 24 h post fertilisation (hpf) and 96 hpf. Hatching rate (B) and malformation rate (C) are presented as the frequency of occurrence at 72 hpf and 96 hpf, respectively. Data are presented as mean and were assessed using two-way ANOVA followed by Bonferroni's post-hoc test. Heart rate data (D), coiling activity (E), distance (F) and velocity (G) are presented as mean ± the standard deviation (SD) and were analysed using Kruskal-Wallis test. The confidence limit of * $p < 0.05$ was considered as statistically significant. The *p* values and *n* size are depicted below the graphs.

hpf embryos exhibited an increase in spontaneous contractions upon exposure to the doses of 0.01–5.0 mM (Fig. 4E). There were no significant differences between distance (Fig. 4F) and velocity (Fig. 4G) swam by larvae as compared to control at 96 hpf.

3.2.3. (R,R)-4'-Methoxy-1-naphtylfenoterol induced developmental malformations

(*R*,*R*)-MNFen exhibited around 8-fold higher lethality in comparison with the above-mentioned compounds, resulting in an LC_{50} value equal to 0.65 mM at 96 hpf (Fig. 5A). (*R*,*R*)-MNFen did not significantly delay the hatchability (Fig. 5B), however, was able to induce substantial morphological abnormalities, i.e. cranial and fin malformations, and growth retardation starting from the dose of 0.25 mM (frequency 20 %; Fig. 5C and Fig. S1C). In contrast to the above-described compounds, (*R*,*R*)-MNFen reduced heart beating at nanomolar doses equal to 10 nM and 100 nM, while an increase in heart rate was observed at no point in time (Fig. 5D). The heart rate inhibition associated with an increase in mortality was observed at the dose of 1.0 mM, as well as 0.5 mM and

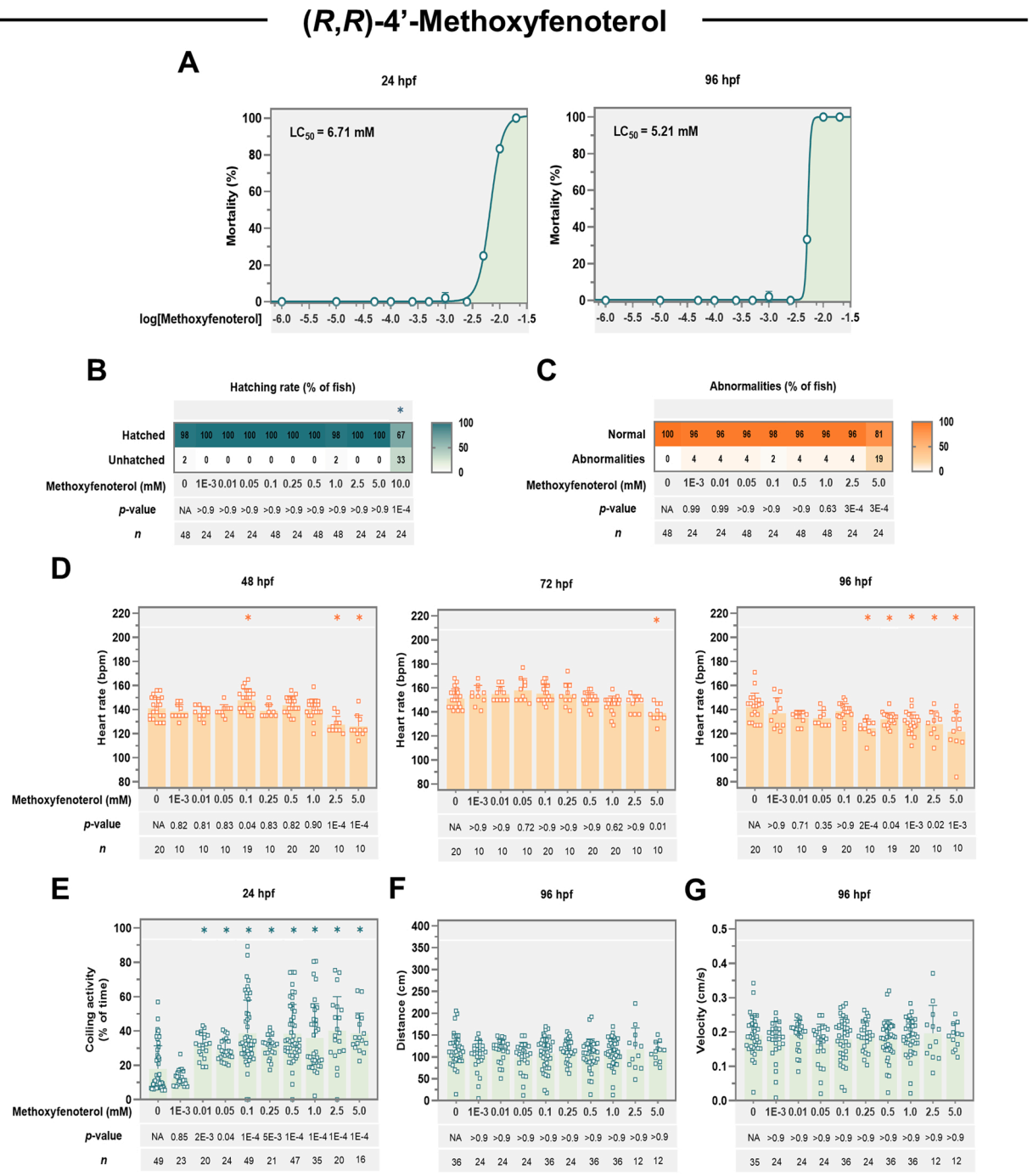

Fig. 4. Toxicity and activity of (*R*,*R*)-4'-methoxyfenoterol in zebrafish. Effects of (*R*,*R*)-MFen on the mortality (A), hatching rate (B), morphological changes (C), heart rate (D), coiling activity (E), distance (F) and velocity (G) swam by larvae. Nonlinear regression was performed on dose-response mortality data (A) at 24 h post fertilisation (hpf) and 96 hpf. Hatching rate (B) and malformation rate (C) are presented as the frequency of occurrence at 72 hpf and 96 hpf, respectively. Data are presented as mean and were assessed using two-way ANOVA followed by Bonferroni's post-hoc test. Data are presented as mean ± the standard deviation (SD) and were analysed using one-way analysis of variance followed by Tukey's post-hoc test (heart rate; D: 48 hpf). Kruskal-Wallis test was used for datasets that failed normality testing or had significantly different variances: heart rate (D: 72 hpf; 96 hpf), coiling activity (E), distance (F) and velocity (G). The confidence limit of * $p < 0.05$ was considered as statistically significant. The *p* values and *n* size are depicted below the graphs.

0.75 mM, at 48 and 72 hpf, respectively. The effect was maintained at doses of 0.25 mM and 0.5 mM at 96 hpf (Fig. 5D). The compound increased the time when embryos were active in a clear dose-dependent manner between 0.005 mM and 0.05 mM doses (Fig. 5E). Then, the embryonic activity returned to the baseline and it was accompanied by an increase in both mortality and the frequency of occurrence of abnormal fish. After 96 h of exposure, (*R*,*R*)-MNFen altered neither distance (Fig. 5F) nor velocity (Fig. 5G) swam by larvae.

3.3. Behavioural assessment of fenoterol and its derivatives

Because the common effects observed after the stimulation of βARs are tremor, anxiety and sympathetic arousal [62], we further evaluated whether similar effects are reflected in a zebrafish model. To assess the effect of fenoterol and its derivatives on locomotor response and anxiety-like behaviour in fish, we adapted an assay that is used to measure anxiety in the rodent models. A thigmotaxic response – the

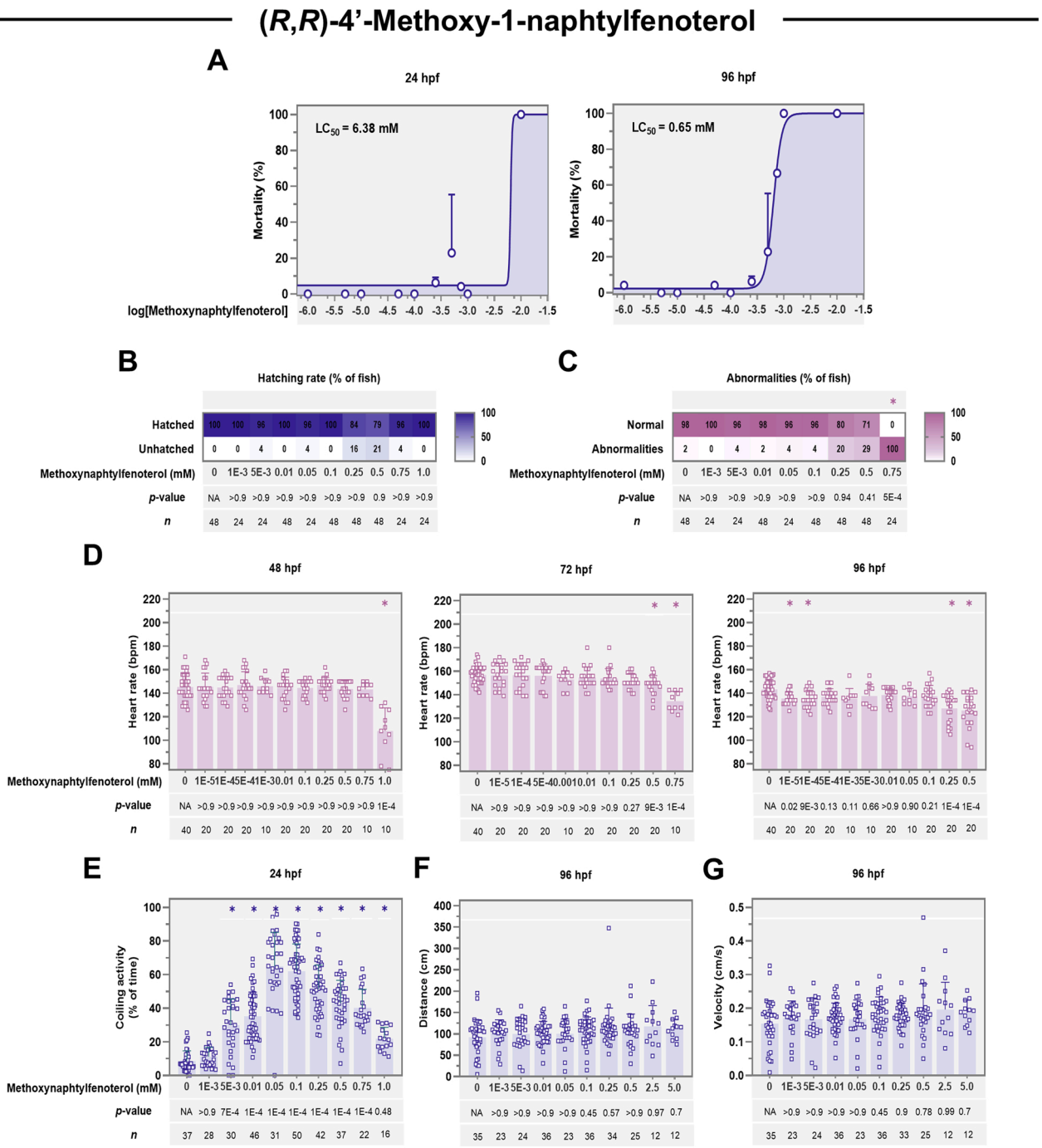

Fig. 5. Toxicity and activity of (*R*,*R*)-4'-methoxy-1-naphtylfenoterol in zebrafish. Effects of (*R*,*R*)-MNFen on the mortality (A), hatching rate (B), morphological changes (C), heart rate (D), coiling activity (E), distance (F) and velocity (G) swam by larvae. Nonlinear regression was performed on dose-response mortality data (A) at 24 h post fertilisation (hpf) and 96 hpf. Hatching rate (B) and malformation rate (C) are presented as the frequency of occurrence at 72 hpf and 96 hpf, respectively. Data are presented as mean and were assessed using two-way ANOVA followed by Bonferroni's post-hoc test. Heart rate data (D), coiling activity (E), distance (F) and velocity (G) are presented as mean ± the standard deviation (SD) and were analysed using Kruskal-Wallis test. The confidence limit of * $p < 0.05$ was considered as statistically significant. The *p* values and *n* size are depicted below the graphs.

tendency to move close to the boundaries and to avoid the centre of the open arena – was used as an index of anxiety. The procedure was enriched with alteration in light and dark conditions, which was proven to elevate an anxiety level in larvae at early developmental stages, demonstrated by a robust increase in a locomotor activity referred to as the visual motor response [38,50].

Our time-course study showed that the distance swam by larvae increased under dark conditions at both 96 and 116 hpf. As expected, the effect stood out at the latter time point in comparison to the former one, and the older fish were more overall active than the younger ones, which stays in line with the literature [63] and can be ascribed to less inflated swim bladder.

The first tested compound – (*R*,*R*)-Fen – elicited no behavioural responses after both 20 h and 40 h of exposure. At the first time point, none of the tested doses affect the total distance swam (Fig. 6A) and the distance moved by larvae in the inner zone (Fig. 6B). After 40 h of exposure, (*R*,*R*)-Fen-treated zebrafish showed no change in locomotor activity (Fig. 6C), and even though the highest tested dose tended to

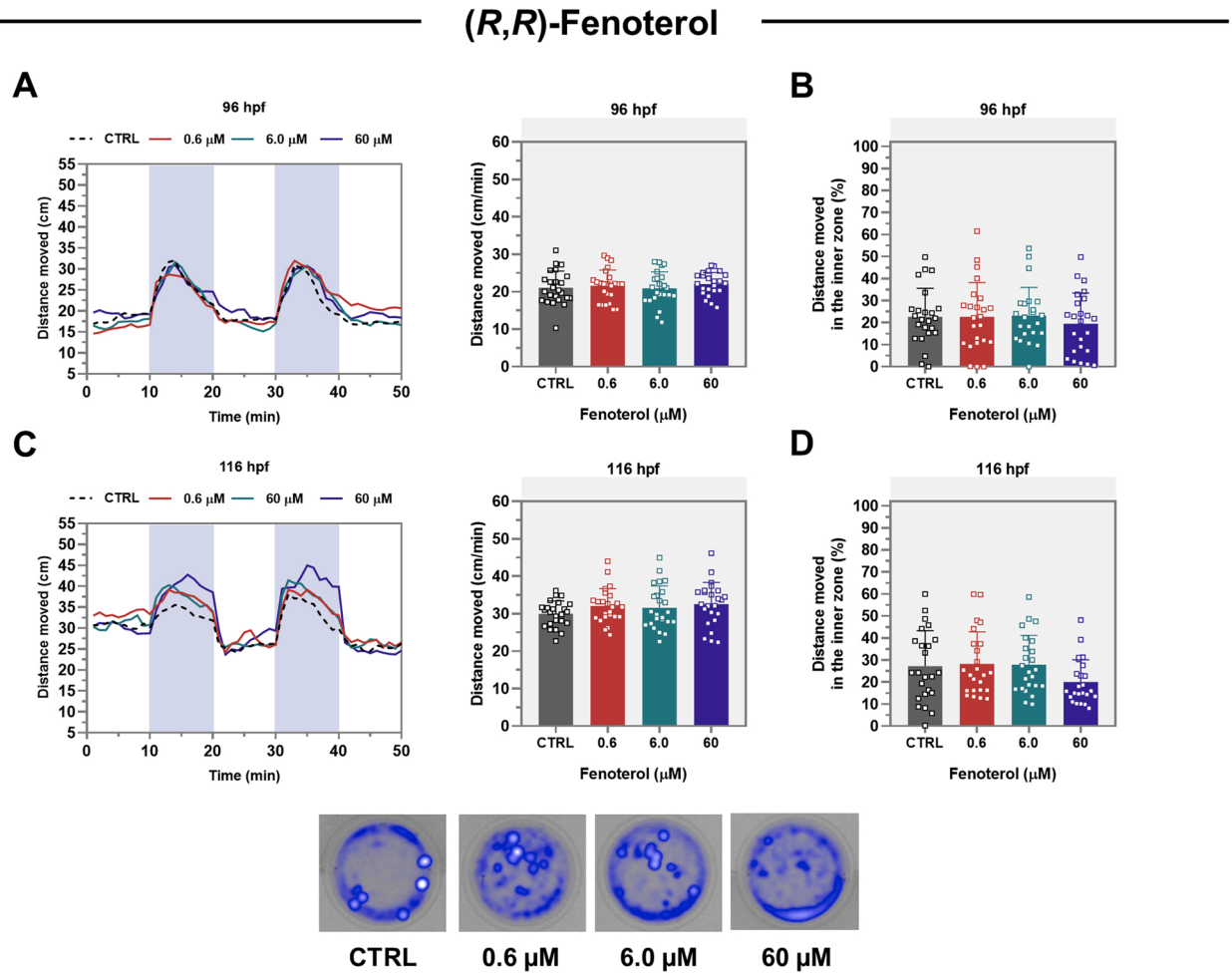

Fig. 6. Behavioural response of (*R*,*R*)-fenoterol in zebrafish. Effects of (*R*,*R*)-Fen on the fish locomotor activity (A) under the light-dark transition test and anxiety-like behaviours (B) measured by the distance swam in the inner zone in 96 h post fertilisation (hpf) larvae. The experiment was repeated at 116 hpf for measuring the locomotor activity (C) and anxiety-like behaviour (D). Data are presented as mean ± the standard deviation (SD). Data were analysed using one-way analysis of variance followed by Tukey's post-hoc test (A, B, C). Kruskal-Wallis test was used for datasets that failed normality testing or had significantly different variances (D). The confidence limit of * $p < 0.05$ was considered as statistically significant. $n = 24$.

increase thigmotaxis, the effect was not statistically significant (Fig. 6D).

(*R*,*R*)-MFen had no effect on fish behaviours at 96 hpf (Fig. 7A and 7B). Further observation revealed that the tested derivative did not change the distance moved by larvae (Fig. 7C), whereas significantly decreased the distance moved by fish in the inner zone at all tested doses of 0.5 µM, 5.0 µM and 50 µM in a clear dose-dependent manner (Fig. 7D), and this indicates an increase in the level of anxiety in fish.

At 96 hpf, acute 20 h of exposure to the next tested compound – (*R*, *R*)-MNFen – did not change locomotor activity nor had an influence on anxiety-like behaviour in larvae (Fig. 8A and B). The next 20 h of exposition to the compound significantly increased the distance moved by larvae at the dose of 6.5 µM (Fig. 8C) and lessened the distance moved in the inner zone at the dose of 0.65 µM and 6.5 µM (Fig. 8D), suggesting a similar anxiogenic property of (*R*,*R*)-MNFen to that observed for (*R*,*R*)-MFen; however, in this case, it cannot be excluded that the effect was ascribed to increased locomotor activity. Representative heatmaps show the anxiety-like behaviour of the individual fish exposed to fenoterol and its derivatives at 116 hpf.

3.4. *β_2ARs are involved in the observed effects of the fenoterol compounds in zebrafish*

To evaluate whether the fenoterol compounds act through β_2ARs in zebrafish, we tested a potent and highly selective β_2AR antagonist – ICI-118,551 – with respect to (*R*,*R*)-Fen. For (*R*,*R*)-Fen the cardio-stimulatory dose of 0.01 mM was selected, based on the toxicological studies (Fig. 3). For ICI-118,551, a minimum inhibitory heart rate concentration (i.e. 0.025 mM) and sub-effective concentration (0.01 mM) were selected, based on our preliminary dose-ranging study (Fig. 9A). We observed here that (*R*,*R*)-Fen significantly increased the heart rate and the effect was reversed after exposure to both concentrations of ICI-118,551 (Fig. 9B), confirming an implication of β_2ARs in the observed effects of the fenoterol compounds.

3.5. *Molecular docking*

3.5.1. *General mechanism of agonist binding to zebrafish β_2ARs*

The structure of the zebrafish β_2AR molecule has not yet been resolved, the two alternative homology models were used instead (see the Methods section for details). For sake of consciousness in the main article contains only the results obtained for models relying on the PDB:3SN6 structure of human β_2AR (Table S1). The results obtained for the PDB:7BZ2-based models are given in Supporting Information (Table S2). Nevertheless, the differences between those two types of models are of rather minor magnitude and both lead to qualitatively the same conclusions.

All studied agonists molecules are arranged in the binding cavity of both β_2AR structures (subtypes A and B) in a similar manner, i.e. the

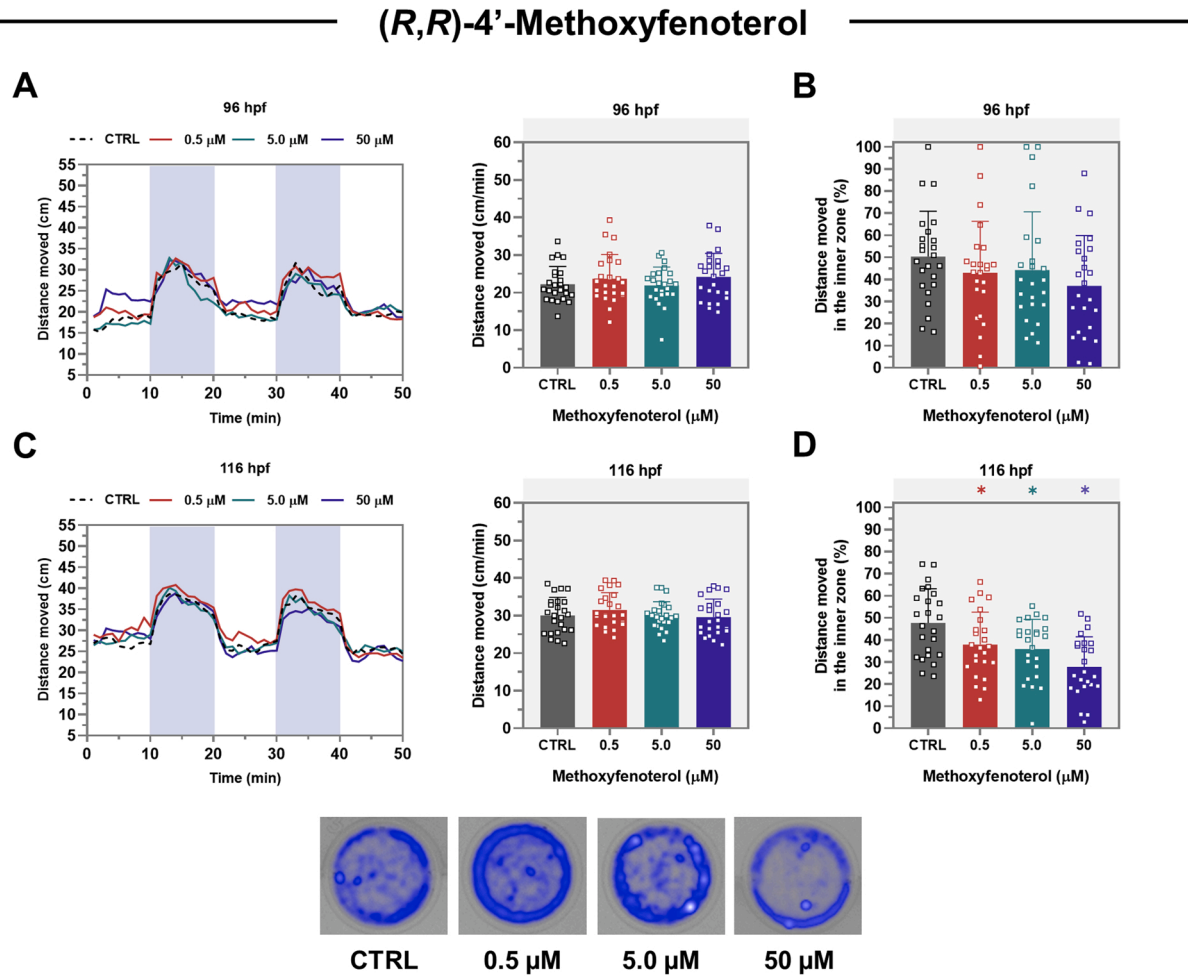

Fig. 7. Behavioural response of (*R*,*R*)-4'-methoxyfenoterol in zebrafish. Effects of (*R*,*R*)-MFen on the fish locomotor activity (A) under the light-dark transition test and anxiety-like behaviours (B) measured by the distance swam in the inner zone in 96 h post fertilisation (hpf) larvae. The experiment was repeated at 116 hpf for measuring the locomotor activity (C) and anxiety-like behaviour (D). Data are presented as mean ± the standard deviation (SD). Data were analysed using one-way analysis of variance followed by Tukey's post-hoc test (B, C, D). Kruskal Wallis test was used for datasets that failed normality testing or had significantly different variances (A). The confidence limit of * $p < 0.05$ was considered as statistically significant. $n = 24$.

individual functional groups (the amine and the hydroxyl moieties) adopt the same orientation in the binding cavity (see Fig. 10). Such qualitatively similar poses agree with the experimentally-resolved position of a series of different ligands in a binding cavity of the human β_2AR; for instance: (i) agonists: adrenaline (PDB 4LDO), formoterol (PDB: 7BZ2), BI-167107 (PDB: 4LDE) and isoprenaline (PDB: 7DHR); inverse agonist: salbutamol (PDB: 7DHI); and (iii) antagonist: timolol (PDB: 6PS6), propranolol (PDB: 6PS5) and alprenolol (PDB: 3NYA) [53,60,64–66]. This clearly demonstrates that the general pattern of interactions between the agonist molecules and β_2AR is conserved within the collective group of human and zebrafish receptors. The results obtained for all docked ligands were presented in Supplemental Information (Tables S1 and S2).

3.5.2. Interactions of fenoterol and its derivatives with subtype A of β_2AR (β_{2A}AR)

In general, the pattern of interactions between fenoterol or its derivatives ((*R*,*R*)-MFen and (*R*,*R*)-MNFen) and zebrafish β_{2A}AR is similar to that observed for the same compounds bound by human β_2AR, as described in our earlier works [67–69]. When focusing on the structural details of the ligand-receptor contacts, we found that the most important and conserved interaction is the ionic bridge between the protonated amine moiety of the ligand and the carboxyl moiety of the aspartic acid residue, located on the 3rd transmembrane domain (TM3), $D^{3.32}$ (in the whole text, the amino-acid residues are numbered according to the Ballesteros-Weinstein scheme [70]). In addition, the same protonated amine moiety of (*R*,*R*)-MNFen, contrary to both (*R*,*R*)-Fen and (*R*,*R*)-MFen can interact with $N^{7.39}$ (amine moiety) mainly as hydrogen bond (HB) acceptor (Fig. 11). Another contact involving $D^{3.32}$ is the interaction with the *β*-hydroxyl moiety (*β*-OH) located at the first chiral centre of all fenoterols. However, this interaction was observed only for (*R*,*R*)-Fen (Fig. 11). It is worth emphasising that the most energetically favourable arrangement corresponds to the situation when the *β*-OH group of ligand can simultaneously interact with both the carboxyl moiety of $D^{3.32}$ and the amine moiety of $N^{7.39}$ as occurred only in this single case (Fig. 11, Table S1). The 3,5-dihydroxyphenyl moiety of all fenoterols creates hydrogen bonds (HBs) with sidechains of serines $S^{5.42}$ and $S^{5.46}$ located on TM5. In addition, HB between the 3,5-dihydroxyphenyl moiety and $N^{6.55}$ was observed but only for (*R*,*R*)-Fen (Fig. 11). The *N*-alkyl chain of (*R*,*R*)-Fen lies close to F188 located on the second extracellular loop (ECL2), $Y^{2.64}$ (TM2) and $W^{3.28}$ (TM3). The *N*-alkyl chain of fenoterol analogues is directed towards mainly $F^{7.35}$, thus the *π*-*π* interactions between the aromatic groups of (*R*,*R*)-MFen or (*R*,*R*)-MNFen and the phenyl ring of $F^{7.35}$ can be created (Fig. 11). Different orientations of the methyl moiety located at the second chiral centre of fenoterol analogues can be observed, e.g. the methyl moiety of (*R*,*R*)-Fen is directed towards $W^{3.28}$ but in the case of (*R*,*R*)-MFen and (*R*,*R*)-MNFen the same group is closer to F188 (ECL2) (Fig. 11).

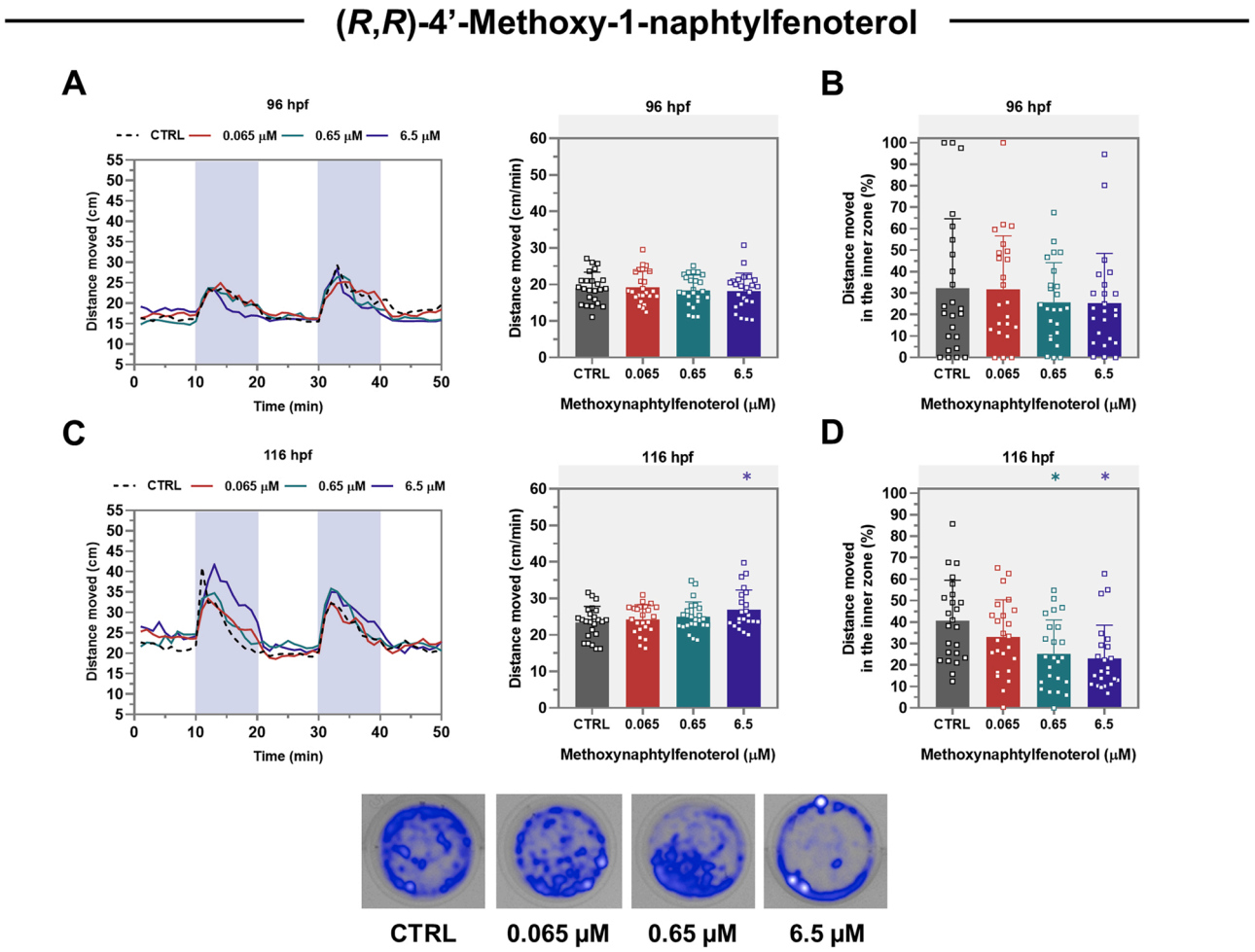

Fig. 8. Behavioural response of (*R*,*R*)-4'-methoxy-1-naphtylfenoterol in zebrafish. Effects of (*R*,*R*)-MNFen on the fish locomotor activity (A) under the light-dark transition test and anxiety-like behaviours (B) measured by the distance swam in the inner zone in 96 h post fertilisation (hpf) larvae. The experiment was repeated at 116 hpf for measuring the locomotor activity (C) and anxiety-like behaviour (D). Data are presented as mean ± the standard deviation (SD). Data were analysed using one-way analysis of variance followed by Tukey's post-hoc test (A, C). Kruskal Wallis test was used for datasets that failed normality testing or had significantly different variances (B, D). The confidence limit of * $p < 0.05$ was considered as statistically significant. $n = 23–24$.

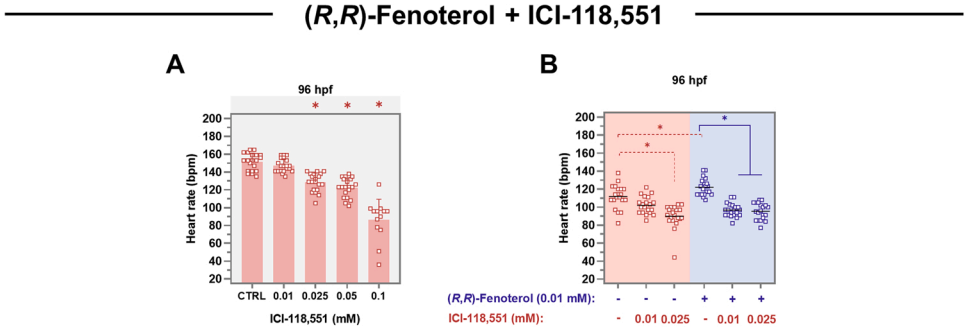

Fig. 9. The role of β_2ARs in (*R*,*R*)-fenoterol-mediated effects. The concentrations of a highly selective β_2AR antagonist – ICI 118,551 – were selected based on our preliminary dose-ranging study (A). Effect of ICI-118,551 against (*R*,*R*)-Fen-induced tachycardia after 24 h exposure (B). Data are presented as ± the standard deviation (SD; A) or mean (B) and were assessed using Kruskal–Wallis test (A) or two-way ANOVA followed by Bonferroni's post-hoc test (B). The confidence limit of * $p < 0.05$ was considered as statistically significant. The difference between control solution and (*R*,*R*)-Fen or ICI-118,551 is depicted by a dashed line, whereas the difference between (*R*,*R*)-Fen alone and the co-administration of (*R*,*R*)-Fen and ICI-118,551 is depicted by a solid line. $n = 13–20$.

The lowest binding energy was obtained in the case of (*R*,*R*)-Fen (−9.9 kcal/mol). For (*R*,*R*)-MFen (−8.8 kcal/mol) and (*R*,*R*)-MNFen (−9.1 kcal/mol) slightly higher binding energies were observed, indicating that these derivatives bind to the receptor with smaller affinity comparing to (*R*,*R*)-Fen (Table S2). Apart from that, all calculated binding energies suggest very high ligand-receptor affinities.

3.5.3. *Interactions of fenoterol and its derivatives with subtype B of β_2AR (β_{2B}AR)*

The general pattern of the orientation of the ligand in the binding cavity as well as the majority of the most essential interactions are analogous as those described as characteristic of subtype A. However, in contrary to subtype A of zebrafish β_2AR, in the case of subtype B the docked ligands are located deeper in the binding pocket of the receptor

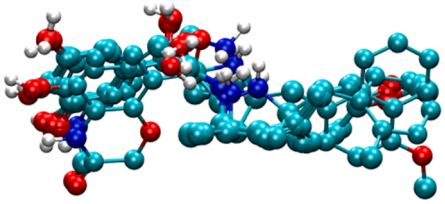

Fig. 10. The superposition of all most energetically-favourable structures of ligands in the binding cavity of zebrafish β_2AR (subtype B).

and locater closer to TM7. The simultaneous interactions of *β*-OH and the protonated amine moiety of fenoterols with both $D^{3.32}$ and $N^{7.39}$ were observed (Fig. 12). Apparently, such an enhanced network of contacts is not explicitly correlated with more favourable ligand-receptor interactions expressed in terms of binding energies (see the next paragraph). A further difference between subtypes A and B is that now the 3,5-dihydroxyphenyl ring of fenoterol derivatives creates the π-π interactions with $F^{6.51}$ (Fig. 12). This residue is a component of the so-called toggle switch, involved in the activation of the human β_2AR [71,72]. A noticeable divergence in the orientation of the *N*-alkyl chain-bound groups of fenoterols can be observed, i.e. 4-hydroxy--phenyl, 4-methoxy-phenyl and 4-methoxy-naphthyl moieties. In the case of (*R*,*R*)-Fen, the 4-hydroxy-phenyl moiety is directed towards TM2 and creates a HB with $Y^{2.64}$. On the other hand, the 4-methoxy-phenyl and 4-methoxy-naphthyl moieties of (*R*,*R*)-MFen and (*R*,*R*)-MNFen, respectively, lie in the neighbourhood of TM7 and may create the π-π interactions with $F^{7.35}$ (Fig. 12).

The determined binding energies are systematically less favourable in comparison to those obtained for the same compounds and subtype A of the receptor. More precisely, the values of −9.4, −8.8 and −10.9 kcal/mol were determined for (*R*,*R*)-Fen, (*R*,*R*)-MFen and (*R*,*R*)-MNFen, respectively. Moreover, the affinity trend is different in comparison to the subtype A.

3.5.4. *Stereoselective binding of fenoterol to zebrafish β_2AR*

The previous subsection contains the results obtained for one stereoisomer of fenoterol ((*R*,*R*)-Fen). When applying the same docking procedure for other stereoisomers of fenoterol ((*S*,*S*)-Fen), we observed a series of differences in a binding pattern that are the result of stereoselective effects. The stereoselective binding was observed for both A and B subtypes of β_2AR.

The protonated amine moiety of ligand interacts simultaneously with $D^{3.32}$ and $N^{7.39}$ only in the case of (*S*,*S*)-Fen (Fig. 13B). In the complex containing (*R*,*R*)-Fen and subtype A of β_2AR the ligand molecule is closer to $D^{3.32}$, which disrupts the potential HBs with $N^{7.39}$ but only allows for the formation of an ionic bridge with the carboxyl moiety of $D^{3.32}$ (Fig. 13A). The second important difference between (*R*,*R*)-Fen and (*S*,*S*)-Fen is that the *β*-OH moiety of (*S*,*S*)-Fen is more distant from $D^{3.32}$ and cannot create a HB with the carboxyl moiety of this residue. In the case of (*R*,*R*)-Fen the *β*-OH moiety can maintain contact with $D^{3.32}$, thus, the unique contribution of $D^{3.32}$ in the receptor-ligand contact may result from the favourable arrangement of the ligand in the orthosteric binding site (Fig. 13A and B).

The arrangement of the methyl group, located at the second chiral centre, is also different in complexes created by (*R*,*R*)-Fen and (*S*,*S*)-Fen. In the case of (*S*,*S*)-Fen interacting with subtype A the methyl group is directed towards $V^{3.33}$. In the case of (*R*,*R*)-Fen the same group is directed towards $W^{3.28}$ and the F188 residue located on ECL2. This divergence is correlated with different arrangements of the *p*-hydroxyphenyl moiety of both compounds; in the case of (*R*,*R*)-Fen it is directed to $Y^{2.64}$ (TM2) or $W^{3.28}$ (TM3), whereas the *p*-hydroxyphenyl group of (*S*,*S*)-Fen lies closer to TM7 and can create the π-π interaction with the phenyl moiety of $F^{7.35}$ which corresponds to tyrosine 308 ($Y^{7.35}$) present in the human β_2AR (Fig. 13A and B). The latter residue has been identified as crucial in the G_s selective effects in ligand-mediated signalling [30].

The stereoselective effects occur also in the case of fenoterol stereoisomers interacting with subtype B of β_2AR. They result in different arrangements of the *p*-hydroxyphenyl groups of particular stereoisomers in the binding pocket. In the case of (*R*,*R*)-Fen, the *p*-hydroxyphenyl moiety interacts with $Y^{2.64}$ or C185 (ECL2) via hydrogen bonding. The same, *p*-hydroxyphenyl moiety of (*S*,*S*)-Fen is located deeper in the binding site and exhibits the π-π interactions involving $Y^{7.43}$. This $Y^{7.43}$ residue corresponds to tyrosine 316 ($Y^{7.43}$) present in the human β_2AR, which participate in the binding of antagonists. Moreover, for β_{2B}AR we

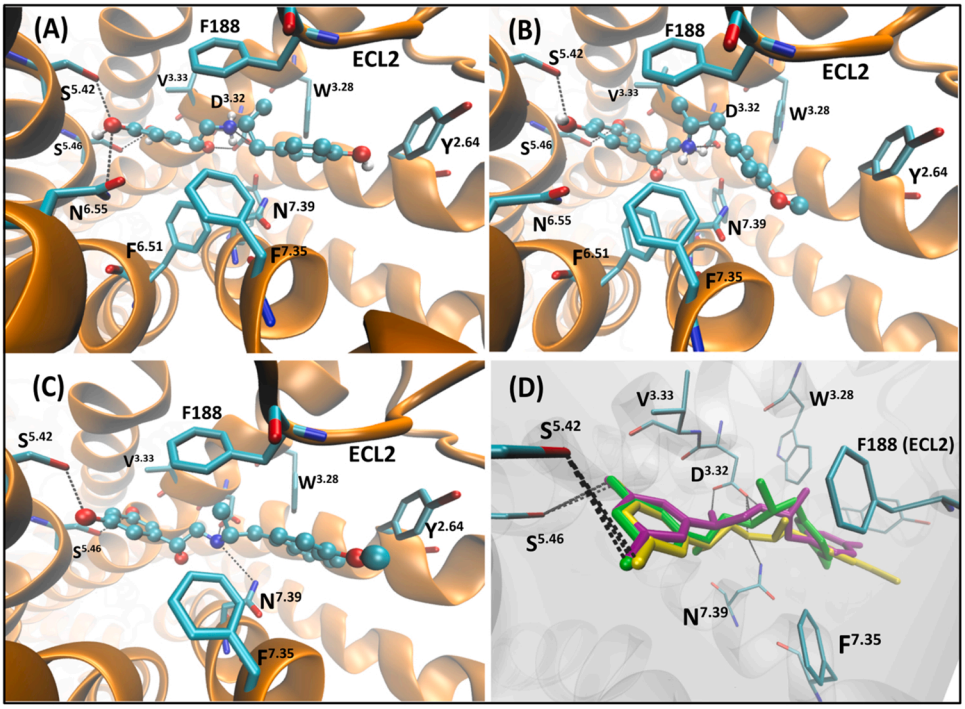

Fig. 11. Graphical illustrations of interactions between (*R*,*R*)-fenoterol (A), (*R*,*R*)-4'-methoxyfenoterol (B) and (*R*,*R*)-4'-methoxy-1-naphtylfenoterol (C) and zebrafish β_{2A}AR (subtype A of β_2AR). Some essential hydrogen bonds involving $Y^{2.64}$, $D^{3.32}$, $S^{5.42}$, $S^{5.46}$, $N^{6.55}$, $N^{7.39}$, $F^{7.35}$ and F188 (ECL2) are highlighted by black, dotted lines. The most important amino acid residues and the ligand molecules are shown in the stick and ball-and-stick representations, respectively (A, B, C). The superposed locations of ligands bound to the receptor: (*R*,*R*)-Fen (purple), (*R*,*R*)-MFen and (*R*,*R*)-MNFen (yellow) (D) (For interpretation of the references to colour in this figure legend, the reader is referred to the web version of this article).

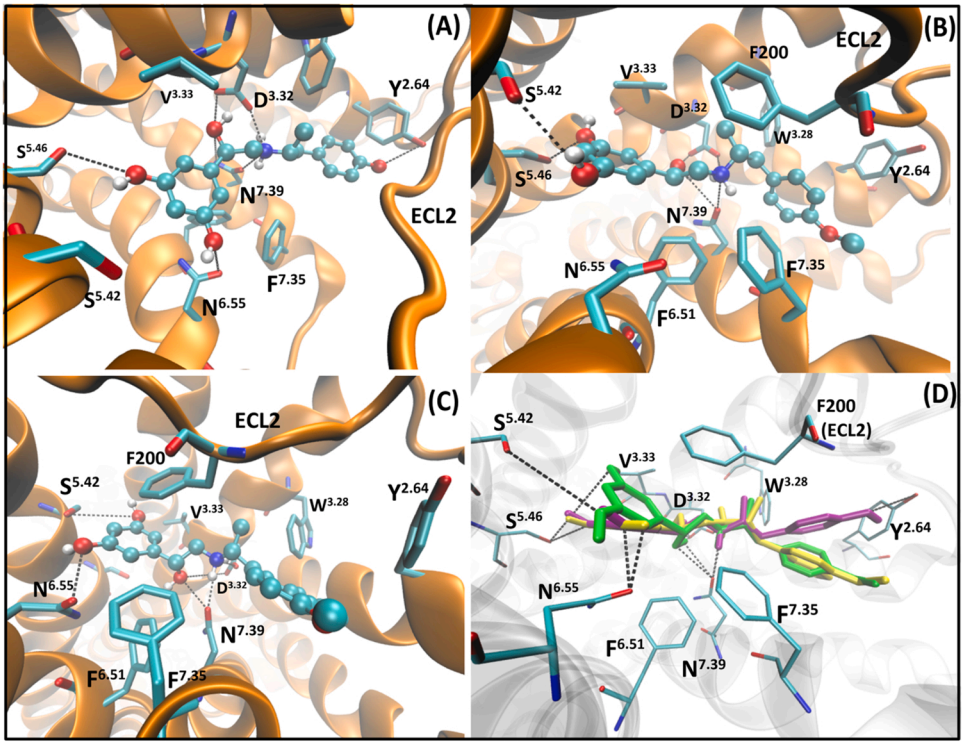

Fig. 12. Graphical illustrations of interactions between (*R*,*R*)- fenoterol (A), (*R*,*R*)-4'-methoxyfenoterol (B) and (*R*,*R*)-4'-methoxy-1-naphtylfenoterol (C) and zebrafish β_{2B}AR (subtype B of β_2AR). Some essential hydrogen bonds involving $Y^{2.64}$, $D^{3.32}$, $S^{5.42}$, $S^{5.46}$, $N^{6.55}$, $N^{7.39}$ and $F^{7.35}$ are highlighted by black, dotted lines. The most important amino acid residues and the ligands molecules are shown in the stick and ball-and-stick representations, respectively (A, B, C). The superposed locations of the ligands bound to the receptor: (*R*,*R*)-Fen (purple), (*R*,*R*)-MFen and (*R*,*R*)-MNFen (yellow) (D) (For interpretation of the references to colour in this figure legend, the reader is referred to the web version of this article).

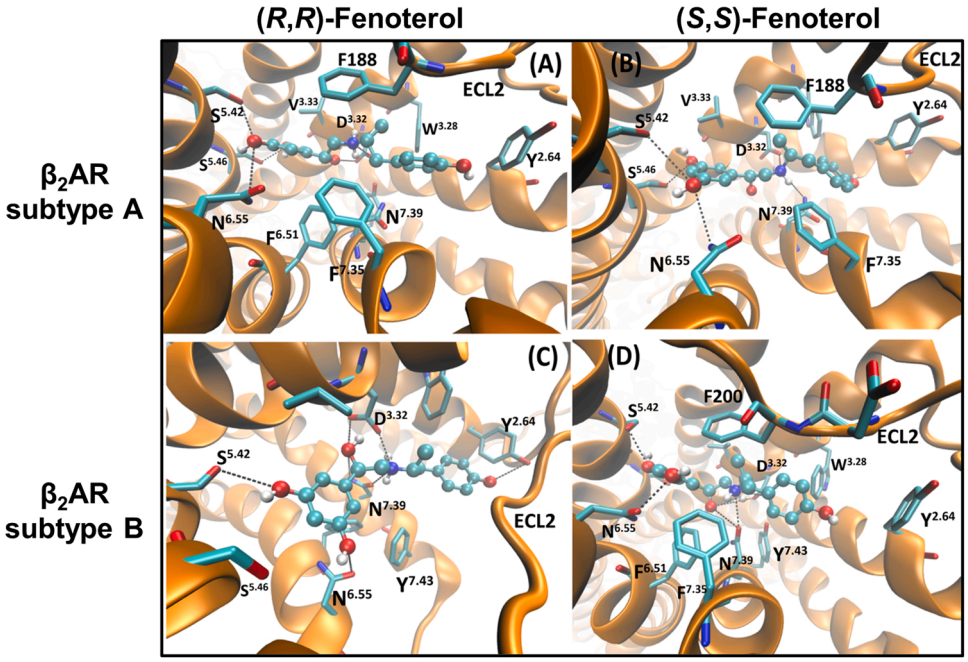

Fig. 13. Graphical illustration of the complexes created by zebrafish β_2AR subtypes A and B with (*R*,*R*)-fenoterol (A, C) and (*S*,*S*)-fenoterol (B, D).

also observed the same tendency in the arrangements of the methyl groups of (*R*,*R*)- and (*S*,*S*)-Fen as in the case of subtype A, e.g. the methyl moiety of (*R*,*R*)-Fen is directed towards $W^{3.28}$ and F200 (ECL2), whereas in the case of (*S*,*S*)-Fen, the same group is directed towards $V^{3.33}$ instead (Fig. 13C and D).

Finally, the binding stereoselectivity demonstrates itself by different binding energy values. For both subtypes of the receptor, the (*S*,*S*)-Fen stereoisomer displays less favourable binding in comparison to (*R*,*R*)-Fen. The corresponding difference is equal to 1.2 kcal/mol in the case of both subtypes of the receptor.

4. Discussion

The presented study is the first demonstration of pharmacological modulation of β_2ARs in zebrafish using full active and selective agonists: fenoterol and its derivatives. Here, we presented toxicological and pharmacological effects observed after exposure to these β_2AR agonists in terms of general toxicity, cardiotoxicity, neurotoxicity and behaviours. Moreover, we described the mechanism of binding of fenoterol and its derivatives to both subtypes of β_2AR (β_{2A}AR and β_{2B}AR) on the molecular level by using the ligand-receptor docking methodology. The

outputs of the research provide detailed insights into the role of zebrafish β_2ARs and can be leveraged towards a better understanding of zebrafish as a novel animal model during the drug discovery process. Also, the presented study speculates about the potential toxicological effects of fenoterol and its derivatives in the therapy.

(*R*,*R*)-Fen is a full agonist with high selectivity towards human β_2AR. It has been demonstrated that the introduction of the new moiety to the fenoterol scaffold increases its affinity for β_2AR and potentiates the stimulation of the receptor [19]. Here, (*R*,*R*)-Fen elicited relatively low mortality resulting in LC_{50} value equal to 5.58 mM, indicating lower toxicity of (*R*,*R*)-Fen in comparison to its derivatives, i.e. (*R*,*R*)-MFen and (*R*,*R*)-MNFen. The introduction of methoxy group resulted in only a slight increase in embryo mortality (LC_{50} = 5.21 mM), whereas an additional methoxynaphtyl group exacerbated toxicity around 8-times in comparison to the parent compound (LC_{50} = 0.65 mM) demonstrating its significant role in toxic actions. There are at least two arising options why an additional methoxynaphtyl moiety determinates higher toxicity in fish. One of them could be that mortality directly depends on the lipophilicity of tested compounds. The most common method to treat embryonic zebrafish is to immerse animals in solution; therefore, water solubility and lipophilicity determine the absorption through the fish skin, and then internal concentrations [73]. Exchange of the hydroxyphenyl group present in (*R*,*R*)-Fen into metoxynaptyl moiety is correlated with the drastically increased log *P* value (1.22 vs 2.96 according to the theoretical predictions of KOWWIN (Estimation Programs Interface Suite™ for Microsoft® Windows, v. 4.11. The United States Environmental Protection Agency, Washington, DC, USA)). Our previous work [74] shows that mortality and lipophilicity of βAR ligands are well correlated, i.e. more lipophilic compounds displayed higher toxicity. The highest lipophilicity of (*R*,*R*)-MNFen might, therefore, trigger higher mortality in comparison with other tested compounds. On the other hand, we previously demonstrated that exposure to nonselective βAR agents caused lethality at higher doses compared to selective β_2AR, as well as a racemic mixture of the (*R*,*R*)/(*S*,*S*)-Fen produced around a 1.9-fold lower mortality rate to that observed here for (*R*,*R*)-Fen [74]. It has been shown that (*R*,*R*)-isomers have a higher affinity for β_2AR and thus are more effective to stimulate β_2AR in humans in comparison to its racemate [25]. A similar effect was observed here. Theoretical investigations demonstrated that (*R*,*R*)-Fen exhibits stronger binding either to subtype A or B of β_2AR in comparison to its stereoisomer (*S*,*S*)-Fen. The corresponding differences in binding energies are equal to 1.2 kcal/mol. Therefore, one could speculate that a more robust activation of one or both forms of β_2ARs led to an increase in fish mortality.

An impairment of early development and weak motor skills contribute to the delay of fish hatchability [75,76]. We observed here that both (*R*,*R*)-Fen and (*R*,*R*)-MFen reduced the hatching rate of fish in 72 hpf. Since no significant abnormalities were noticeable after the (*R*,*R*)-Fen exposure, the effect may be related to the altered movement of embryos. A similar delay in hatching was observed for (*R*,*R*)-MFen; however, it cannot be excluded that in this case the observed effect was associated with a high mortality rate. It is further interesting to note that while we did not observe any malformations after (*R*,*R*)-Fen exposure, the treatment with this β_2AR agonist induced considerable inhibition of pigment synthesis. A similar effect was observed for (*R*,*R*)/(*S*,*S*)-Fen [74], nonetheless compared with the racemic mixture the effect was more marked for (*R*,*R*)-Fen, confirming a superior activity in β_2ARs stimulation of (*R*,*R*)-isomer to that of racemate also in zebrafish. In the research of Wang and co-authors [41], the knock-down of β_2ARs by morpholino oligonucleotides revealed the functional importance of β_{2A}AR in pigmentation. This suggests that (*R*,*R*)-Fen, which exhibits depigmentation properties, should interact stronger with β_{2A}AR in comparison to either (*S*,*S*)-Fen, racemic mixture or fenoterol derivatives. Indeed, the docking results reflected this expectation, showing the most favourable binding energy for (*R*,*R*)-Fen interacting with β_{2A}AR, exceeding those obtained for (*S*,*S*)-Fen, (*R*,*R*)-MFen and (*R*,*R*)-MNFen by 1.2, 1.1 and 0.8 kcal/mol, respectively. The competition effects present in the case of the racemic mixture of fenoterols may reduce the number of the (*R*,*R*)-Fen-β_{2A}AR complexes and diminish the depigmentation magnitude. Thus, the stereoselective depigmentation can be explained on the ground of ligand-receptor interaction strength. However, some alternative explanations may be proposed, also based on the docking results. For instance, (*R*,*R*)-Fen is the only compound for which the interaction with TM2 (namely: with $Y^{2.64}$) was observed. This may suggest the slightly different conformational response contributing to the further stages of signalling process and the final depigmentation effect. The hypotheses about depigmentation occurring via diverse signalling mechanisms induced by (*R*,*R*)-Fen and (*S*,*S*)-Fen is additionally supported by experimental findings related to human β_2AR. Both stereoisomers differ in their selectivity towards G protein and induced signalling paths; (*R*,*R*)-Fen is G_s-selective whereas (*S*,*S*)-Fen is not selective and may activate both G_s and G_i proteins [30]. Although it is impossible to state if the same mechanisms hold for zebrafish β_{2A}AR, the differences between ligand-receptor interactions observed in our docking studies allow speculating about that. Moreover, it is worth noting that human β_2AR and both zebrafish β_{2A}AR and β_{2B}AR share another feature related to interactions with stereoisomers of fenoterol. Namely, both theoretical and experimental studies demonstrated that (*R*,*R*)-Fen interacts much stronger with human β_2AR in comparison to (*S*,*S*)-Fen [19,25,67].

In comparison to the parent compound, (*R*,*R*)-MFen did not cause any apparent morphological abnormalities, whereas (*R*,*R*)-MNFen induced severe alteration of cranial and tail developments at higher concentrations. Wang and co-authors [44] revealed that β_1AR and β_{2B}AR are the main βARs that regulate body axis straightening in zebrafish, and demonstrated that the knock-down of β_{2B}AR produced a severe ventral curly axis phenotype. Thus, (*R*,*R*)-MNFen-induced malformations may be ascribed to the modulation of β_{2B}AR in embryonic zebrafish. This effect can be explained by significantly stronger interactions of (*R*,*R*)-MNFen with β_{2B}AR in comparison to (*R*,*R*)-Fen or (*R*,*R*)-MFen, as indicated by docking study; the corresponding binding energies are equal to −10.9, −9.4 and −9.1 kcal/mol, respectively. Moreover, the different patterns of interactions of the *N*-alkyl chain and its substituents with receptor observed for (*R*,*R*)-MFen and (*R*,*R*)-MNFen may be responsible for diverse conformational responses.

Our previous works confirmed that the pharmacological response of the β-adrenergic system is well conserved across species [74,77]. Both βAR agonists and antagonists closely mimicked the cardiac effects observed in mammalian models [74] and βAR blockers were able to ameliorate heart dysfunctions under various heart failure-based approaches [77]. In humans, β_2AR is involved in the regulation of cardiovascular functions via the stimulatory G_s protein and the inhibitory G_i protein. Stimulation of β_2AR leads to an increase in cardiac contractility and heart rhythm; however, its persistent activation may cause a reversal of the effects [1]. In zebrafish, all βARs couple the stimulatory G_s protein, whereas one or both forms of zebrafish β_2ARs may reduce cardiac functions by interacting with G_i protein [42]. Recently, Joyce and colleagues [78] proved that the chronotropic effect of adrenergic stimulation persists even in the β_1AR knock-out fish, likely due to the upregulation of other βAR subtypes. Consistent with this hypothesis is our previous observation that selective β_2AR agonists are able to boost heart rate, albeit at higher doses compared to nonselective ones, and this may be a consequence of larger expression of β_1AR in comparison to β_2ARs in zebrafish heart [41]. We observed here that (*R*,*R*)-Fen and (*R*,*R*)-MFen initially increased heart rate; i.e. (*R*,*R*)-Fen at 72 hpf and (*R*,*R*)-MFen even earlier at 48 hpf, however, at the higher dose. An increase in heart rate was observed at 125-times lower dose for (*R*,*R*)-Fen in comparison with the racemic micture of (*R*,*R*)/(*S*,*S*)-Fen [74], confirming that (*R*,*R*)-isomer is more potent to stimulate β_2ARs also in zebrafish. Moreover, our docking study indicated that (*R*,*R*)-Fen interacts more intensively with β_{2B}AR in comparison to (*S*,*S*)-Fen. The crucial difference in this context is the arrangement of the

p-hydroxyphenyl group. In the case of (*R*,*R*)-Fen this group created HB with $Y^{2.64}$, whereas in the case of (*S*,*S*)-Fen it forms HB with $Y^{7.43}$, i.e. the residue the counterpart of which is responsible for antagonist binding in the human receptor. In sharp contrast, the third tested compound – (*R*,*R*)-MNFen, which is the most selective β_2AR out of the tested agonists ($K_{i\ \beta 1AR}/K_{i\ \beta 2AR} = 573$ [19]), suppressed heart rhythm at nanomolar doses after 96 h of exposure, suggesting that its higher affinity for the zebrafish β_{2B}AR than for either β_1AR or β_{2A}AR might be involved in this inhibitory effect. One could also speculate that this effect was associated with the stimulation of the inhibitory G_i protein of the zebrafish β_{2B}AR.

Our time-course study imitated a clinical phenomenon, wherein prolonged exposure to drugs induces toxicological effects. As cardiotoxicity directly depends on exposure level, we compared how zebrafish heart responds to the drugs at higher tested doses after 96 h of exposure. Comparing the ratio between the lowest dose that caused heart rate suppression and the dose that was lethal for 50% of animals, it is clearly noticed that (*R*,*R*)-MFen reduced heart rate at the widest range of concentrations, i.e. the inhibitory dose was 21-times lower than LC_{50} value, indicating its cardiotoxic potential. Both (*R*,*R*)-Fen and (*R*,*R*)-MNFen treatments also reduced heart rhythm, however, to a lesser extent; the suppressive doses were around 2.2-times and 2.6-times lower than the LC_{50} value, respectively. As discussed before, β_2AR agonists at higher doses lose selectivity for β_2AR, and an increased risk of adverse cardiovascular events might be associated with their action at the β_1AR [5], thus one could speculate that (*R*,*R*)-MFen may display smaller selectivity towards zebrafish β_2AR vs β_1AR in comparison with remaining fenoterols. The docking simulations confirmed this by indicating that (*R*,*R*)-MFen exhibits the weakest interactions with β_2AR among all fenoterols except of (*S*,*S*)-Fen (Table S1). Whilst it has been previously shown that fenoterol is able to activate β_3AR in humans [21], we did not consider the role of the zebrafish β_3ARs in the fenoterols-related effects. β_3ARs have only been found in zebrafish blood, and this is, therefore, unlikely that these receptors play a significant role in the presented study. Moreover, we further showed that a highly selective β_2AR antagonist – ICI-118,551 – was able to antagonise the (*R*,*R*)-Fen-induced tachycardia suggesting that the β_2ARs are indeed involved in the observed effects of the fenoterol compounds in zebrafish.

The most common dose-dependent sympathomimetic side effect observed during the βAR agonist therapy is tremor and anxiety [79]. Non-selective βAR agonists, adrenaline [80] and isoprenaline [81] as well as selective β_2AR, salbutamol [82], have been known to induce tremors by increasing muscle activity, changing the gain of muscle receptors and spinal reflex loops, mediated via peripherally located β_2AR; βAR blockers are able to alleviate these effects [83]. In zebrafish muscle both variants of β_2ARs are predominant receptors; however, β_{2B}AR is expressed to a greater extent [41]. In our study, all tested β_2AR agonists increased coiling activity after 24 h of exposure, suggesting increased activity in primary motor neurons [84] after exposure to non-toxic doses. A further increase of (*R*,*R*)-Fen and (*R*,*R*)-MNFen concentrations decreased the motor behaviour. It has been proved that early embryonic movements provide an accessible readout for testing how chemicals interfere with the developing nervous system and therefore can serve as useful early endpoints of neurotoxicity [84]. Among the tested compounds, (*R*,*R*)-Fen started to reduce embryonic movement at a dose that was around 22-times lower than the LC_{50} value, suggesting its toxic effects on either the motor or nervous systems. The observation is consistent with the above-described decline in hatchability after (*R*,*R*)-Fen exposure, which might be related to poor motor skills. A similar failure was observed after (*R*,*R*)-MNFen exposure; however, the effect was associated with an increase in mortality rate, while (*R*,*R*)-MFen caused no drop in embryonic movements, which may suggest little or lack of neurotoxicity from both compound exposures. To further find out how prolong exposure to fenoterol derivatives changes spontaneous swimming in fish, the distance and velocity swam by 96 hpf larvae were analysed under continuous light conditions. We observed here that none of the tested compounds altered distance nor velocity swam, therefore, no alteration in fish locomotion has been found [84].

The widespread and abundant distribution of β_2AR in the brain suggests an important role of this receptor in the central nervous system. The β_2AR expression has been reported in neurons of the cerebellum [85], hippocampus [86] and amygdala [87] in mammalian models. In the zebrafish brain, subtype A of β_2AR is mostly expressed [41]. Extensive evidence points out that the stimulation of the sympathetic system modulates locomotion and anxiety state in humans [79,88], whereas neuropharmacological effects of β-adrenergic stimulation in fish are defined vaguely. Few studies demonstrated that the mode of action of adrenergic ligands is reflected in fish and seems to be conserved across the species. Noradrenaline – endogenous catecholamine – is essential to promote wakefulness and arousal in fish [89]. Isoprenaline – a non-selective βAR agonist – has been shown to stimulate the photomotor response and act as a potent anxiogenic agent in zebrafish embryos and larvae [90]. Propranolol – βAR antagonist – is able to block behavioural effects mediated by βAR agonists [90,91]. To further reveal the specific role of β_2AR in anxiety behaviour, we decided to test the fenoterol compounds. A common outcome of the tested compounds was the induction of an anxiety state in fish and this supports the notion that β-adrenergic neural response is a highly conserved intraspecies. Furthermore, our findings suggest a more complex role of β_2ARs in the modulation of anxiety-related behaviours in zebrafish. Among the tested compounds only (*R*,*R*)-Fen-treated zebrafish exhibited no behavioural effect. Consistent with the above, since (*R*,*R*)-Fen displayed a higher affinity for β_{2A}AR than for β_{2B}AR, and β_{2A}AR are mainly distributed in zebrafish brain [41], the anxiogenic behaviour might be, therefore, mediated through the peripheral action. As expected, both (*R*,*R*)-MFen and (*R*,*R*)-MNFen showed an anxiogenic-like effect, but in the case of (*R*,*R*)-MNFen it can be attributed to changes in locomotor activity. Loss of selectivity towards β_2ARs leading to dysregulation of β-adrenergic transmission might arise as one of the proposed mechanisms of the observed anxiety-like behaviour if (*R*,*R*)-MFen is considered. Whereas, due to the highest affinity of (*R*,*R*)-MNFen for the β_{2B}AR, which is expressed mainly in fish muscle [41], an increase in locomotion and therefore an intensification of anxiety level could be observed.

5. Conclusions

In this study, we comprehensively clarify the role of β_2ARs in the modulation of toxicological and behavioural effects in zebrafish, with a particular emphasis on the distinct roles of subtypes A and B in the observed effects. Selective agonists – fenoterol and its derivatives – were used as new model compounds because of their well-described high affinity for β_2AR along with their growing potential in the therapy of a broad range of disorders. Our results indicate that: (i) functional response of the β_2AR is highly conserved intraspecies; (ii) (*R*,*R*)-isomers are more potent to stimulate zebrafish β_2ARs than (*S*,*S*)-isomers; (iii) (*R*,*R*)-Fen displays the highest affinity for subtype A of zebrafish β_2AR. β_{2A}AR might be involved in pigment depletion and regulates a neurotoxic effect at early stages; (iv) (*R*,*R*)-MFen shows the lowest affinity for zebrafish β_2ARs out of the tested fenoterols and this might be associated with its cardiotoxic effect; (vi) (*R*,*R*)-MNFen displays the highest affinity for subtype B of zebrafish β_2AR and modulation of this receptor might be associated with the development of malformations and causes a negative chronotropic effect; (v) β-adrenergic stimulation induces anxiety-like behaviours in zebrafish. Taken together, the presented data offer insights into the functional responses of the zebrafish β_2ARs, and support the value of the zebrafish model in pharmacological and toxicological research.

Funding sources

This work was supported by the National Science Centre, Poland [2017/25/B/NZ7/02654].

CRediT authorship contribution statement

Monika Maciag: Conceptualization, Data curation, Formal analysis, Investigation, Methodology, Validation, Visualization, Writing – original draft, Writing – review & editing. **Wojciech Plazinski:** Data curation, Formal analysis, Investigation, Methodology, Validation, Visualization, Writing – original draft, Writing – review & editing. **Wojciech Pulawski:** Investigation, Methodology, Validation. **Michal Kolinski:** Investigation, Methodology, Validation. **Krzysztof Jozwiak:** Writing – review & editing. **Anita Plazinska:** Conceptualization, Formal analysis, Investigation, Methodology, Validation, Visualization, Writing – original draft, Writing – review & editing, Funding acquisition, Project administration.

Conflict of interest statement

No competing interests declared.

Data availability

The data that support the findings of this study are available from the corresponding author upon reasonable request. Some data may not be made available because of privacy or ethical restrictions.

Acknowledgement

The authors thank Agnieszka Michalak for preparing a graphical abstract created with BioRender.com.

Appendix A. Supporting information

Supplementary data associated with this article can be found in the online version at doi:10.1016/j.biopha.2023.114355.

References

[1] A. Lymperopoulos, G. Rengo, W.J. Koch, Adrenergic nervous system in heart failure: pathophysiology and therapy, Circ. Res. 113 (6) (2013) 739–753, https://doi.org/10.1161/CIRCRESAHA.113.300308.
[2] S.F. Steinberg, Beta1-adrenergic receptor regulation revisited, Circ. Res. 123 (11) (2018) 1199–1201, https://doi.org/10.1161/CIRCRESAHA.118.313884.
[3] K.M. Rambacher, N.H. Moniri, The beta2-adrenergic receptor-ROS signaling axis: an overlooked component of beta2AR function? Biochem Pharmacol. 171 (2020), 113690 https://doi.org/10.1016/j.bcp.2019.113690.
[4] D.E. Berkowitz, N.A. Nardone, R.M. Smiley, D.T. Price, D.K. Kreutter, R. T. Fremeau, D.A. Schwinn, Distribution of beta 3-adrenoceptor mRNA in human tissues, Eur. J. Pharmacol. 289 (2) (1995) 223–228, https://doi.org/10.1016/0922-4106(95)90098-5.
[5] D.M. Williams, B.K. Rubin, Clinical pharmacology of bronchodilator medications, Respir. Care 63 (6) (2018) 641–654, https://doi.org/10.4187/respcare.06051.
[6] Y. Song, C. Xu, J. Liu, Y. Li, H. Wang, D. Shan, I.W. Wainer, X. Hu, Y. Zhang, A. Y. Woo, R.P. Xiao, Heterodimerization with 5-HT2BR is indispensable for beta2AR-mediated cardioprotection, Circ. Res. 128 (2) (2021) 262–277, https://doi.org/10.1161/CIRCRESAHA.120.317011.
[7] B. Mravec, L. Horvathova, L. Hunakova, Neurobiology of cancer: the role of beta-adrenergic receptor signaling in various tumor environments, Int. J. Mol. Sci. 21 (21) (2020), https://doi.org/10.3390/ijms21217958.
[8] F.L. Baker, A.B. Bigley, N.H. Agha, C.R. Pedlar, D.P. O'Connor, R.A. Bond, C. M. Bollard, E. Katsanis, R.J. Simpson, Systemic beta-adrenergic receptor activation augments the ex vivo expansion and anti-tumor activity of Vgamma9Vdelta2 T-cells, Front. Immunol. 10 (2019) 3082, https://doi.org/10.3389/fimmu.2019.03082.
[9] A. Kalinovich, N. Dehvari, A. Aslund, S. van Beek, C. Halleskog, J. Olsen, E. Forsberg, E. Zacharewicz, G. Schaart, M. Rinde, A. Sandstrom, R. Berlin, C. G. Ostenson, J. Hoeks, T. Bengtsson, Treatment with a beta-2-adrenoceptor agonist stimulates glucose uptake in skeletal muscle and improves glucose homeostasis, insulin resistance and hepatic steatosis in mice with diet-induced obesity, Diabetologia 63 (8) (2020) 1603–1615, https://doi.org/10.1007/s00125-020-05171-y.
[10] M. Hostrup, J. Onslev, The beta2 -adrenergic receptor - a re-emerging target to combat obesity and induce leanness? J. Physiol. 600 (5) (2022) 1209–1227, https://doi.org/10.1113/JP281819.
[11] L. Peterson, K.P. Ismond, E. Chapman, P. Flood, Potential benefits of therapeutic use of beta2-adrenergic receptor agonists in neuroprotection and Parkinsonmus disease, J. Immunol. Res. 2014 (2014), 103780, https://doi.org/10.1155/2014/103780.
[12] W. Wang, M. Xu, Y.Y. Zhang, B. He, Fenoterol, a beta(2)-adrenoceptor agonist, inhibits LPS-induced membrane-bound CD14, TLR4/CD14 complex, and inflammatory cytokines production through beta-arrestin-2 in THP-1 cell line, Acta Pharmacol. Sin. 30 (11) (2009) 1522–1528, https://doi.org/10.1038/aps.2009.153.
[13] T. Keranen, T. Hommo, M. Hamalainen, E. Moilanen, R. Korhonen, Anti-inflammatory effects of beta2-receptor agonists salbutamol and terbutaline are mediated by MKP-1, PLoS One 11 (2) (2016), e0148144, https://doi.org/10.1371/journal.pone.0148144.
[14] Y. Izumi, H. Okatani, M. Shiota, T. Nakao, R. Ise, G. Kito, K. Miura, H. Iwao, Effects of metoprolol on epinephrine-induced takotsubo-like left ventricular dysfunction in non-human primates, Hypertens. Res. 32 (5) (2009) 339–346, https://doi.org/10.1038/hr.2009.28.
[15] S.Y. Shin, T. Kim, H.S. Lee, J.H. Kang, J.Y. Lee, K.H. Cho, D.H. Kim, The switching role of beta-adrenergic receptor signalling in cell survival or death decision of cardiomyocytes, Nat. Commun. 5 (2014) 5777, https://doi.org/10.1038/ncomms6777.
[16] A. Wnorowski, M. Sadowska, R.K. Paul, N.S. Singh, A. Boguszewska-Czubara, L. Jimenez, K. Abdelmohsen, L. Toll, K. Jozwiak, M. Bernier, I.W. Wainer, Activation of beta2-adrenergic receptor by (R,R')-4'-methoxy-1-naphthylfenoterol inhibits proliferation and motility of melanoma cells, Cell Signal. 27 (5) (2015) 997–1007, https://doi.org/10.1016/j.cellsig.2015.02.012.
[17] M. Bernier, J. Catazaro, N.S. Singh, A. Wnorowski, A. Boguszewska-Czubara, K. Jozwiak, R. Powers, I.W. Wainer, GPR55 receptor antagonist decreases glycolytic activity in PANC-1 pancreatic cancer cell line and tumor xenografts, Int. J. Cancer 141 (10) (2017) 2131–2142, https://doi.org/10.1002/ijc.30904.
[18] A. Wnorowski, J. Such, R.K. Paul, R.P. Wersto, F.E. Indig, K. Jozwiak, M. Bernier, I. W. Wainer, Concurrent activation of beta2-adrenergic receptor and blockage of GPR55 disrupts pro-oncogenic signaling in glioma cells, Cell Signal. 36 (2017) 176–188, https://doi.org/10.1016/j.cellsig.2017.05.006.
[19] K. Jozwiak, A.Y. Woo, M.J. Tanga, L. Toll, L. Jimenez, J.A. Kozocas, A. Plazinska, R.P. Xiao, I.W. Wainer, Comparative molecular field analysis of fenoterol derivatives: A platform towards highly selective and effective beta(2)-adrenergic receptor agonists, Bioorg. Med. Chem. 18 (2) (2010) 728–736, https://doi.org/10.1016/j.bmc.2009.11.062.
[20] J.G. Baker, The selectivity of beta-adrenoceptor agonists at human beta1-, beta2- and beta3-adrenoceptors, Br. J. Pharmacol. 160 (5) (2010) 1048–1061, https://doi.org/10.1111/j.1476-5381.2010.00754.x.
[21] S. Palea, M. Rekik, C. Rouget, P. Camparo, H. Botto, P. Rischmann, P. Lluel, T. D. Westfall, Fenoterol functionally activates the beta(3)-adrenoceptor in human urinary bladder, comparison with rat and mouse: implications for drug discovery, Eur. J. Pharmacol. 690 (1–3) (2012) 202–206, https://doi.org/10.1016/j.ejphar.2012.06.036.
[22] B.R. Erdogan, Z.E. Yesilyurt, E. Arioglu-Inan, M.C. Michel, Validation of fenoterol to study beta2-adrenoceptor function in the rat urinary bladder, Pharmacology 107 (1–2) (2022) 116–121, https://doi.org/10.1159/000519720.
[23] H. Wang, Y. Chen, H. Zhu, S. Wang, X. Zhang, D. Xu, K. Cao, J. Zou, Increased response to beta(2)-adrenoreceptor stimulation augments inhibition of IKr in heart failure ventricular myocytes, PLoS One 7 (9) (2012), e46186, https://doi.org/10.1371/journal.pone.0046186.
[24] D.G. Kiely, R.I. Cargill, A. Grove, A.D. Struthers, B.J. Lipworth, Abnormal myocardial repolarisation in response to hypoxaemia and fenoterol, Thorax 50 (10) (1995) 1062–1066, https://doi.org/10.1136/thx.50.10.1062.
[25] K. Jozwiak, C. Khalid, M.J. Tanga, I. Berzetei-Gurske, L. Jimenez, J.A. Kozocas, A. Woo, W. Zhu, R.P. Xiao, D.R. Abernethy, I.W. Wainer, Comparative molecular field analysis of the binding of the stereoisomers of fenoterol and fenoterol derivatives to the beta2 adrenergic receptor, J. Med. Chem. 50 (12) (2007) 2903–2915, https://doi.org/10.1021/jm070030d.
[26] K. Jozwiak, A. Plazinska, L. Toll, L. Jimenez, A.Y. Woo, R.P. Xiao, I.W. Wainer, Effect of fenoterol stereochemistry on the beta2 adrenergic receptor system: ligand-directed chiral recognition, Chirality 23 (Suppl 1) (2011) E1–E6, https://doi.org/10.1002/chir.20963.
[27] A. Lymperopoulos, Arrestins in the cardiovascular system: an update, Prog. Mol. Biol. Transl. Sci. 159 (2018) 27–57, https://doi.org/10.1016/bs.pmbts.2018.07.003.
[28] V.L. Desimine, K.A. McCrink, B.M. Parker, S.L. Wertz, J. Maning, A. Lymperopoulos, Biased agonism/antagonism of cardiovascular GPCRs for heart failure therapy, Int. Rev. Cell Mol. Biol. 339 (2018) 41–61, https://doi.org/10.1016/bs.ircmb.2018.02.007.
[29] A.Y. Woo, X.Y. Ge, L. Pan, G. Xing, Y.M. Mo, R.J. Xing, X.R. Li, Y.Y. Zhang, I. W. Wainer, M.S. Cheng, R.P. Xiao, Discovery of beta-arrestin-biased beta(2)-adrenoceptor agonists from 2-amino-2-phenylethanol derivatives, Acta Pharmacol. Sin. 40 (8) (2019) 1095–1105, https://doi.org/10.1038/s41401-018-0200-x.
[30] A.Y. Woo, K. Jozwiak, L. Toll, M.J. Tanga, J.A. Kozocas, L. Jimenez, Y. Huang, Y. Song, A. Plazinska, K. Pajak, R.K. Paul, M. Bernier, I.W. Wainer, R.P. Xiao, Tyrosine 308 is necessary for ligand-directed Gs protein-biased signaling of beta2-adrenoceptor, J. Biol. Chem. 289 (28) (2014) 19351–19363, https://doi.org/10.1074/jbc.M114.558882.
[31] E.E. Patton, L.I. Zon, D.M. Langenau, Zebrafish disease models in drug discovery: from preclinical modelling to clinical trials, Nat. Rev. Drug Discov. 20 (8) (2021) 611–628, https://doi.org/10.1038/s41573-021-00210-8.
[32] Y.M. Bradford, S. Toro, S. Ramachandran, L. Ruzicka, D.G. Howe, A. Eagle, P. Kalita, R. Martin, S.A. Taylor Moxon, K. Schaper, M. Westerfield, Zebrafish

models of human disease: gaining insight into human disease at ZFIN, ILAR J. 58 (1) (2017) 4–16, https://doi.org/10.1093/ilar/ilw040.
[33] K. Howe, M.D. Clark, C.F. Torroja, J. Torrance, C. Berthelot, M. Muffato, J. E. Collins, S. Humphray, K. McLaren, L. Matthews, S. McLaren, I. Sealy, M. Caccamo, C. Churcher, C. Scott, J.C. Barrett, R. Koch, G.J. Rauch, S. White, W. Chow, B. Kilian, L.T. Quintais, J.A. Guerra-Assuncao, Y. Zhou, Y. Gu, J. Yen, J. H. Vogel, T. Eyre, S. Redmond, R. Banerjee, J. Chi, B. Fu, E. Langley, S.F. Maguire, G.K. Laird, D. Lloyd, E. Kenyon, S. Donaldson, H. Sehra, J. Almeida-King, J. Loveland, S. Trevanion, M. Jones, M. Quail, D. Willey, A. Hunt, J. Burton, S. Sims, K. McLay, B. Plumb, J. Davis, C. Clee, K. Oliver, R. Clark, C. Riddle, D. Elliot, G. Threadgold, G. Harden, D. Ware, S. Begum, B. Mortimore, G. Kerry, P. Heath, B. Phillimore, A. Tracey, N. Corby, M. Dunn, C. Johnson, J. Wood, S. Clark, S. Pelan, G. Griffiths, M. Smith, R. Glithero, P. Howden, N. Barker, C. Lloyd, C. Stevens, J. Harley, K. Holt, G. Panagiotidis, J. Lovell, H. Beasley, C. Henderson, D. Gordon, K. Auger, D. Wright, J. Collins, C. Raisen, L. Dyer, K. Leung, L. Robertson, K. Ambridge, D. Leongamornlert, S. McGuire, R. Gilderthorp, C. Griffiths, D. Manthravadi, S. Nichol, G. Barker, S. Whitehead, M. Kay, J. Brown, C. Murnane, E. Gray, M. Humphries, N. Sycamore, D. Barker, D. Saunders, J. Wallis, A. Babbage, S. Hammond, M. Mashreghi-Mohammadi, L. Barr, S. Martin, P. Wray, A. Ellington, N. Matthews, M. Ellwood, R. Woodmansey, G. Clark, J. Cooper, A. Tromans, D. Grafham, C. Skuce, R. Pandian, R. Andrews, E. Harrison, A. Kimberley, J. Garnett, N. Fosker, R. Hall, P. Garner, D. Kelly, C. Bird, S. Palmer, I. Gehring, A. Berger, C.M. Dooley, Z. Ersan-Urun, C. Eser, H. Geiger, M. Geisler, L. Karotki, A. Kirn, J. Konantz, M. Konantz, M. Oberlander, S. Rudolph-Geiger, M. Teucke, C. Lanz, G. Raddatz, K. Osoegawa, B. Zhu, A. Rapp, S. Widaa, C. Langford, F. Yang, S.C. Schuster, N.P. Carter, J. Harrow, Z. Ning, J. Herrero, S.M. Searle, A. Enright, R. Geisler, R.H. Plasterk, C. Lee, M. Westerfield, P.J. de Jong, L.I. Zon, J.H. Postlethwait, C. Nusslein-Volhard, T.J. Hubbard, H. Roest Crollius, J. Rogers, D.L. Stemple, The zebrafish reference genome sequence and its relationship to the human genome, Nature 496 (7446) (2013) 498–503, https://doi.org/10.1038/nature12111.
[34] E.E. Patton, D.M. Tobin, Spotlight on zebrafish: the next wave of translational research, Dis. Model. Mech. 12 (3) (2019), https://doi.org/10.1242/dmm.039370.
[35] C.L. Winata, S. Korzh, I. Kondrychyn, V. Korzh, Z. Gong, The role of vasculature and blood circulation in zebrafish swimbladder development, BMC Dev. Biol. 10 (2010) 3, https://doi.org/10.1186/1471-213X-10-3.
[36] A.V. Kalueff, M. Gebhardt, A.M. Stewart, J.M. Cachat, M. Brimmer, J.S. Chawla, C. Craddock, E.J. Kyzar, A. Roth, S. Landsman, S. Gaikwad, K. Robinson, E. Baatrup, K. Tierney, A. Shamchuk, W. Norton, N. Miller, T. Nicolson, O. Braubach, C.P. Gilman, J. Pittman, D.B. Rosemberg, R. Gerlai, D. Echevarria, E. Lamb, S.C. Neuhauss, W. Weng, L. Bally-Cuif, H. Schneider, C. Zebrafish Neuroscience Research, Towards a comprehensive catalog of zebrafish behavior 1.0 and beyond, Zebrafish 10 (1) (2013) 70–86, https://doi.org/10.1089/zeb.2012.0861.
[37] S. Cassar, I. Adatto, J.L. Freeman, J.T. Gamse, I. Iturria, C. Lawrence, A. Muriana, R.T. Peterson, S. Van Cruchten, L.I. Zon, Use of zebrafish in drug discovery toxicology, Chem. Res. Toxicol. 33 (1) (2020) 95–118, https://doi.org/10.1021/acs.chemrestox.9b00335.
[38] M. Maciag, A. Michalak, K. Skalicka-Wozniak, M. Zykubek, A. Ciszewski, B. Budzynska, Zebrafish and mouse models for anxiety evaluation - A comparative study with xanthotoxin as a model compound, Brain Res. Bull. 165 (2020) 139–145, https://doi.org/10.1016/j.brainresbull.2020.09.024.
[39] B.D. Fontana, M.O. Parker, The larval diving response (LDR): validation of an automated, high-throughput, ecologically relevant measure of anxiety-related behavior in larval zebrafish (Danio rerio, J. Neurosci. Methods (2022), 109706, https://doi.org/10.1016/j.jneumeth.2022.109706.
[40] P. Panula, Y.C. Chen, M. Priyadarshini, H. Kudo, S. Semenova, M. Sundvik, V. Sallinen, The comparative neuroanatomy and neurochemistry of zebrafish CNS systems of relevance to human neuropsychiatric diseases, Neurobiol. Dis. 40 (1) (2010) 46–57, https://doi.org/10.1016/j.nbd.2010.05.010.
[41] Z. Wang, Y. Nishimura, Y. Shimada, N. Umemoto, M. Hirano, L. Zang, T. Oka, C. Sakamoto, J. Kuroyanagi, T. Tanaka, Zebrafish beta-adrenergic receptor mRNA expression and control of pigmentation, Gene 446 (1) (2009) 18–27, https://doi.org/10.1016/j.gene.2009.06.005.
[42] S.L. Steele, X. Yang, M. Debiais-Thibaud, T. Schwerte, B. Pelster, M. Ekker, M. Tiberi, S.F. Perry, In vivo and in vitro assessment of cardiac beta-adrenergic receptors in larval zebrafish (Danio rerio), J. Exp. Biol. 214 (Pt 9) (2011) 1445–1457, https://doi.org/10.1242/jeb.052803.
[43] P. Perdikaris, C.R. Dermon, Behavioral and neurochemical profile of MK-801 adult zebrafish model: Forebrain beta2-adrenoceptors contribute to social withdrawal and anxiety-like behavior, Prog. Neuropsychopharmacol. Biol. Psychiatry 115 (2022), 110494, https://doi.org/10.1016/j.pnpbp.2021.110494.
[44] X. Wang, S. Wang, Z. Meng, C. Zhao, Adrb1 and Adrb2b are the major beta-adrenergic receptors regulating body axis straightening in zebrafish, J. Genet. Genom. 47 (12) (2020) 781–784, https://doi.org/10.1016/j.jgg.2020.10.009.
[45] OECD. (2013). *Test No. 236: Fish Embryo Acute Toxicity (FET) Test.*
[46] A. Swaminathan, R. Hassan-Abdi, S. Renault, A. Siekierska, R. Riche, M. Liao, P.A. M. de Witte, C. Yanicostas, N. Soussi-Yanicostas, P. Drapeau, E. Samarut, Non-canonical mTOR-Independent Role of DEPDC5 in regulating GABAergic network development, Curr. Biol. 28 (12) (2018) 1924–1937.e1925, https://doi.org/10.1016/j.cub.2018.04.061.
[47] H. Richendrfer, S.D. Pelkowski, R.M. Colwill, R. Creton, On the edge: pharmacological evidence for anxiety-related behavior in zebrafish larvae, Behav. Brain Res. 228 (1) (2012) 99–106, https://doi.org/10.1016/j.bbr.2011.11.041.
[48] D.J. Davis, E.C. Bryda, C.H. Gillespie, A.C. Ericsson, Microbial modulation of behavior and stress responses in zebrafish larvae, Behav. Brain Res. 311 (2016) 219–227, https://doi.org/10.1016/j.bbr.2016.05.040.
[49] K.B. Tierney, Behavioural assessments of neurotoxic effects and neurodegeneration in zebrafish, Biochim. Biophys. Acta 1812 (3) (2011) 381–389, https://doi.org/10.1016/j.bbadis.2010.10.011.
[50] S.J. Schnorr, P.J. Steenbergen, M.K. Richardson, D.L. Champagne, Measuring thigmotaxis in larval zebrafish, Behav. Brain Res. 228 (2) (2012) 367–374, https://doi.org/10.1016/j.bbr.2011.12.016.
[51] C. UniProt, UniProt: the universal protein knowledgebase in 2021, Nucleic Acids Res. 49 (D1) (2021) D480–D489, https://doi.org/10.1093/nar/gkaa1100.
[52] S.G. Rasmussen, B.T. DeVree, Y. Zou, A.C. Kruse, K.Y. Chung, T.S. Kobilka, F. S. Thian, P.S. Chae, E. Pardon, D. Calinski, J.M. Mathiesen, S.T. Shah, J.A. Lyons, M. Caffrey, S.H. Gellman, J. Steyaert, G. Skiniotis, W.I. Weis, R.K. Sunahara, B. K. Kobilka, Crystal structure of the beta2 adrenergic receptor-Gs protein complex, Nature 477 (7366) (2011) 549–555, https://doi.org/10.1038/nature10361.
[53] Y. Zhang, F. Yang, S. Ling, P. Lv, Y. Zhou, W. Fang, W. Sun, L. Zhang, P. Shi, C. Tian, Single-particle cryo-EM structural studies of the beta2AR-Gs complex bound with a full agonist formoterol, Cell Discov. 6 (2020) 45, https://doi.org/10.1038/s41421-020-0176-9.
[54] S.G. Rasmussen, H.J. Choi, J.J. Fung, E. Pardon, P. Casarosa, P.S. Chae, B. T. Devree, D.M. Rosenbaum, F.S. Thian, T.S. Kobilka, A. Schnapp, I. Konetzki, R. K. Sunahara, S.H. Gellman, A. Pautsch, J. Steyaert, W.I. Weis, B.K. Kobilka, Structure of a nanobody-stabilized active state of the beta(2) adrenoceptor, Nature 469 (7329) (2011) 175–180, https://doi.org/10.1038/nature09648.
[55] M.A. Larkin, G. Blackshields, N.P. Brown, R. Chenna, P.A. McGettigan, H. McWilliam, F. Valentin, I.M. Wallace, A. Wilm, R. Lopez, J.D. Thompson, T. J. Gibson, D.G. Higgins, W. Clustal, X. Clustal, version 2.0, Bioinformatics 23 (21) (2007) 2947–2948, https://doi.org/10.1093/bioinformatics/btm404.
[56] B. Webb, A. Sali, Comparative protein structure modeling using MODELLER, Curr. Protoc. Bioinform. 54 (2016) 5 6 1–5 6 37, https://doi.org/10.1002/cpbi.3.
[57] M.D. Hanwell, D.E. Curtis, D.C. Lonie, T. Vandermeersch, E. Zurek, G.R. Hutchison, Avogadro: an advanced semantic chemical editor, visualization, and analysis platform, J. Chemin. 4 (1) (2012) 17, https://doi.org/10.1186/1758-2946-4-17.
[58] A.K. Rappe, C.J. Casewit, K.S. Colwell, W.A. Goddard, W.M. Skiff, UFF, a full periodic table force field for molecular mechanics and molecular dynamics simulations, J. Am. Chem. Soc. 114 (25) (1992) 10024–10035, https://doi.org/10.1021/ja00051a040.
[59] O. Trott, A.J. Olson, AutoDock Vina: improving the speed and accuracy of docking with a new scoring function, efficient optimization, and multithreading, J. Comput. Chem. 31 (2) (2010) 455–461, https://doi.org/10.1002/jcc.21334.
[60] A.M. Ring, A. Manglik, A.C. Kruse, M.D. Enos, W.I. Weis, K.C. Garcia, B.K. Kobilka, Adrenaline-activated structure of beta2-adrenoceptor stabilized by an engineered nanobody, Nature 502 (7472) (2013) 575–579, https://doi.org/10.1038/nature12572.
[61] R. von Hellfeld, P. Pannetier, T. Braunbeck, Specificity of time- and dose-dependent morphological endpoints in the fish embryo acute toxicity (FET) test for substances with diverse modes of action: the search for a "fingerprint", Environ. Sci. Pollut. Res. Int. 29 (11) (2022) 16176–16192, https://doi.org/10.1007/s11356-021-16354-4.
[62] A.R. Teed, J.S. Feinstein, M. Puhl, R.C. Lapidus, V. Upshaw, R.T. Kuplicki, J. Bodurka, O.A. Ajijola, W.H. Kaye, W.K. Thompson, M.P. Paulus, S.S. Khalsa, Association of generalized anxiety disorder with autonomic hypersensitivity and blunted ventromedial prefrontal cortex activity during peripheral adrenergic stimulation: a randomized clinical trial, JAMA Psychiatry 79 (4) (2022) 323–332, https://doi.org/10.1001/jamapsychiatry.2021.4225.
[63] R.M. Colwill, R. Creton, Locomotor behaviors in zebrafish (Danio rerio) larvae, Behav. Process. 86 (2) (2011) 222–229, https://doi.org/10.1016/j.beproc.2010.12.003.
[64] A. Ishchenko, B. Stauch, G.W. Han, A. Batyuk, A. Shiriaeva, C. Li, N. Zatsepin, U. Weierstall, W. Liu, E. Nango, T. Nakane, R. Tanaka, K. Tono, Y. Joti, S. Iwata, I. Moraes, C. Gati, V. Cherezov, Toward G protein-coupled receptor structure-based drug design using X-ray lasers, IUCrJ 6 (Pt 6) (2019) 1106–1119, https://doi.org/10.1107/S2052252519013137.
[65] F. Yang, S. Ling, Y. Zhou, Y. Zhang, P. Lv, S. Liu, W. Fang, W. Sun, L.A. Hu, L. Zhang, P. Shi, C. Tian, Different conformational responses of the β2-adrenergic receptor-Gs complex upon binding of the partial agonist salbutamol or the full agonist isoprenaline, Natl. Sci. Rev. 8 (9) (2020), https://doi.org/10.1093/nsr/nwaa284.
[66] D. Wacker, G. Fenalti, M.A. Brown, V. Katritch, R. Abagyan, V. Cherezov, R. C. Stevens, Conserved binding mode of human beta2 adrenergic receptor inverse agonists and antagonist revealed by X-ray crystallography, J. Am. Chem. Soc. 132 (33) (2010) 11443–11445, https://doi.org/10.1021/ja105108q.
[67] A. Plazinska, M. Kolinski, I.W. Wainer, K. Jozwiak, Molecular interactions between fenoterol stereoisomers and derivatives and the beta(2)-adrenergic receptor binding site studied by docking and molecular dynamics simulations, J. Mol. Model 19 (11) (2013) 4919–4930, https://doi.org/10.1007/s00894-013-1981-y.
[68] L. Toll, K. Pajak, A. Plazinska, K. Jozwiak, L. Jimenez, J.A. Kozocas, M.J. Tanga, J. E. Bupp, I.W. Wainer, Thermodynamics and docking of agonists to the beta(2)-adrenoceptor determined using [(3)H](R,R')-4-methoxyfenoterol as the marker ligand, Mol. Pharmacol. 81 (6) (2012) 846–854, https://doi.org/10.1124/mol.111.077347.
[69] A. Plazinska, W. Plazinski, K. Jozwiak, Agonist binding by the beta2-adrenergic receptor: an effect of receptor conformation on ligand association-dissociation characteristics, Eur. Biophys. J. 44 (3) (2015) 149–163, https://doi.org/10.1007/s00249-015-1010-4.

[70] J.A. Ballesteros, H. Weinstein, [19] Integrated methods for the construction of three-dimensional models and computational probing of structure-function relations in G protein-coupled receptors, in: S.C. Sealfon (Ed.), Methods in Neurosciences, 25, Academic Press, 1995, pp. 366–428.
[71] S. Bhattacharya, S.E. Hall, H. Li, N. Vaidehi, Ligand-stabilized conformational states of human beta(2) adrenergic receptor: insight into G-protein-coupled receptor activation, Biophys. J. 94 (6) (2008) 2027–2042, https://doi.org/10.1529/biophysj.107.117648.
[72] A. Plazinska, W. Plazinski, R. Luchowski, A. Wnorowski, W. Grudzinski, W. I. Gruszecki, Ligand-induced action of the W286(6.48) rotamer toggle switch in the beta2-adrenergic receptor, Phys. Chem. Chem. Phys. 20 (1) (2017) 581–594, https://doi.org/10.1039/c7cp04808d.
[73] N.S. Sipes, S. Padilla, T.B. Knudsen, Zebrafish: as an integrative model for twenty-first century toxicity testing, Birth Defects Res. C Embryo Today 93 (3) (2011) 256–267, https://doi.org/10.1002/bdrc.20214.
[74] M. Maciag, A. Wnorowski, K. Bednarz, A. Plazinska, Evaluation of β-adrenergic ligands for development of pharmacological heart failure and transparency models in zebrafish, Toxicol. Appl. Pharmacol. (2021), 115812, https://doi.org/10.1016/j.taap.2021.115812.
[75] M.E. Leite-Ferreira, H. Araujo-Silva, A.C. Luchiari, Individual differences in hatching time predict alcohol response in zebrafish, Front. Behav. Neurosci. 13 (2019) 166, https://doi.org/10.3389/fnbeh.2019.00166.
[76] H. Yang, X. Liang, Y. Zhao, X. Gu, Z. Mao, Q. Zeng, H. Chen, C.J. Martyniuk, Molecular and behavioral responses of zebrafish embryos/larvae after sertraline exposure, Ecotoxicol. Environ. Saf. 208 (2021), 111700, https://doi.org/10.1016/j.ecoenv.2020.111700.
[77] M. Maciag, A. Wnorowski, M. Mierzejewska, A. Plazinska, Pharmacological assessment of zebrafish-based cardiotoxicity models, Biomed. Pharmacother. 148 (2022), 112695, https://doi.org/10.1016/j.biopha.2022.112695.
[78] W. Joyce, Y.K. Pan, K. Garvey, V. Saxena, S.F. Perry, Regulation of heart rate following genetic deletion of the ss1 adrenergic receptor in larval zebrafish, Acta Physiol. 235 (4) (2022), e13849, https://doi.org/10.1111/apha.13849.
[79] G. Barisione, M. Baroffio, E. Crimi, V. Brusasco, Beta-adrenergic agonists, Pharmaceuticals 3 (4) (2010) 1016–1044, https://doi.org/10.3390/ph3041016.
[80] C.D. Marsden, T.H. Foley, D.A. Owen, R.G. McAllister, Peripheral beta-adrenergic receptors concerned with tremor, Clin. Sci. 33 (1) (1967) 53–65.
[81] B. Abila, J.F. Wilson, R.W. Marshall, A. Richens, The tremorolytic action of beta-adrenoceptor blockers in essential, physiological and isoprenaline-induced tremor is mediated by beta-adrenoceptors located in a deep peripheral compartment, Br. J. Clin. Pharmacol. 20 (4) (1985) 369–376, https://doi.org/10.1111/j.1365-2125.1985.tb05079.x.
[82] B. Koster, M. Lauk, J. Timmer, T. Winter, B. Guschlbauer, F.X. Glocker, A. Danek, G. Deuschl, C.H. Lucking, Central mechanisms in human enhanced physiological tremor, Neurosci. Lett.. 241 (2–3) (1998) 135–138, https://doi.org/10.1016/s0304-3940(98)00015-9.
[83] M.R. Baker, S.N. Baker, Beta-adrenergic modulation of tremor and corticomuscular coherence in humans, PLoS One 7 (11) (2012), e49088, https://doi.org/10.1371/journal.pone.0049088.
[84] J.A. Fitzgerald, S. Konemann, L. Krumpelmann, A. Zupanic, C. Vom Berg, Approaches to test the neurotoxicity of environmental contaminants in the zebrafish model: from behavior to molecular mechanisms, Environ. Toxicol. Chem. 40 (4) (2021) 989–1006, https://doi.org/10.1002/etc.4951.
[85] C. Gaiddon, Y. Larmet, E. Trinh, A.L. Boutillier, B. Sommer, J.P. Loeffler, Brain-derived neurotrophic factor exerts opposing effects on beta2-adrenergic receptor according to depolarization status of cerebellar neurons, J. Neurochem. 73 (4) (1999) 1467–1476, https://doi.org/10.1046/j.1471-4159.1999.0731467.x.
[86] N.N. Guo, B.M. Li, Cellular and subcellular distributions of beta1- and beta2-adrenoceptors in the CA1 and CA3 regions of the rat hippocampus, Neuroscience 146 (1) (2007) 298–305, https://doi.org/10.1016/j.neuroscience.2007.01.013.
[87] L.L. Qu, N.N. Guo, B.M. Li, Beta1- and beta2-adrenoceptors in basolateral nucleus of amygdala and their roles in consolidation of fear memory in rats, Hippocampus 18 (11) (2008) 1131–1139, https://doi.org/10.1002/hipo.20478.
[88] S.G. Wendell, H. Fan, C. Zhang, G. Protein-Coupled, Receptors in asthma therapy: pharmacology and drug action, Pharmacol. Rev. 72 (1) (2020) 1–49, https://doi.org/10.1124/pr.118.016899.
[89] C. Singh, G. Oikonomou, D.A. Prober, Norepinephrine is required to promote wakefulness and for hypocretin-induced arousal in zebrafish, Elife 4 (2015), e07000, https://doi.org/10.7554/eLife.07000.
[90] P.T. Gauthier, M.M. Vijayan, Nonlinear mixed-modelling discriminates the effect of chemicals and their mixtures on zebrafish behavior, Sci. Rep. 8 (1) (2018) 1999, https://doi.org/10.1038/s41598-018-20112-x.
[91] K. Abbas, F. Saputra, M.E. Suryanto, Y.H. Lai, J.C. Huang, W.H. Yu, K.H. Chen, Y. T. Lin, C.D. Hsiao, Evaluation of effects of ractopamine on cardiovascular, respiratory, and locomotory physiology in animal model zebrafish larvae, Cells 10 (9) (2021), https://doi.org/10.3390/cells10092449.